Journal of Soil Science and Plant Nutrition (2020) 20:105–124
https://doi.org/10.1007/s42729-019-00105-z

ORIGINAL PAPER

24-Epibrassinolide Improves Root Anatomy and Antioxidant Enzymes in Soybean Plants Subjected to Zinc Stress

Lucilene Rodrigues dos Santos[1] · Breno Ricardo Serrão da Silva[1] · Tatiana Pedron[2] · Bruno Lemos Batista[2] · Allan Klynger da Silva Lobato[1]

Received: 19 June 2019 / Accepted: 16 September 2019 / Published online: 22 October 2019

Abstract

The aim of this research was to determine whether 24-epibrassinolide can mitigate oxidative stress in soybean plants subjected to different zinc levels; to examine this, we evaluated the possible repercussions on anatomical, nutritional, biochemical, physiological and morphological behaviours. The experiment followed a completely randomized factorial design with two concentrations of 24-epibrassinolide (0 and 100 nM EBR, described as - EBR and + EBR, respectively) and three zinc supplies (0.2, 20 and 2000 μM Zn, described as low, control and a high supply of Zn). In general, low and high zinc supplies produced deleterious effects. However, plants exposed to high zinc +100 nM EBR presented increases of 25%, 7%, 9% 29% and 69% for root epidermis, root endodermis, root cortex, vascular cylinder and metaxylem, respectively, when compared to the same treatment without the steroid. The steroid spray alleviated the impact produced by zinc stress on nutritional status, and these results were intrinsically linked to incremental changes in root structure, mainly vascular cylinder and metaxylem. Antioxidant enzymes play crucial roles in the photosynthetic machinery of plants treated with 24-epibrassinolide and stressed by high and low zinc supply, modulating reactive oxygen species scavenging and protecting the chloroplast membranes, with clear positive repercussions on photosystem II efficiency and photosynthetic pigments. The stimulation induced by this steroid on gas exchange can be explained by the favourable conditions detected in stomatal performance and leaf anatomy, thus enhancing the diffusion of carbon dioxide.

Keywords 24-epibrassinolide · Antioxidant system · *Glycine max* · Root anatomy · Zinc supply

Abbreviations

APX	Ascorbate peroxidase
BRs	Brassinosteroids
CA	Carbonic anhydrase
CAR	Carotenoids
CAT	Catalase
Chl *a*	Chlorophyll a
Chl *b*	Chlorophyll b
C_i	Intercellular CO_2 concentration
CO_2	Carbon dioxide
E	Transpiration rate
EBR	24-epibrassinolide
EDS	Equatorial diameter of the stomata
EL	Electrolyte leakage
ETAb	Epidermis thickness from abaxial leaf side
ETAd	Epidermis thickness from adaxial leaf side
ETR	Electron transport rate
ETR/P_N	Ratio between the apparent electron transport rate and net photosynthetic rate
EXC	Relative energy excess at the PSII level
F_0	Minimal fluorescence yield of the dark-adapted state
F_m	Maximal fluorescence yield of the dark-adapted state
F_v	Variable fluorescence
F_v/fm	Maximal quantum yield of PSII photochemistry
g_s	Stomatal conductance
H_2O_2	Hydrogen peroxide
LDM	Leaf dry matter
MDA	Malondialdehyde
NPQ	Nonphotochemical quenching
O_2^-	Superoxide

✉ Allan Klynger da Silva Lobato
allanllobato@yahoo.com.br

[1] Núcleo de Pesquisa Vegetal Básica e Aplicada, Universidade Federal Rural da Amazônia, Rodovia PA, Paragominas, Pará 256, Brazil

[2] Centro de Ciências Naturais e Humanas, Universidade Federal do ABC, Santo André, São Paulo, Brazil

PDS	Polar diameter of the stomata
P_N	Net photosynthetic rate
P_N/C_i	Instantaneous carboxylation efficiency
POX	Peroxidase
PPT	Palisade parenchyma thickness
PSII	Photosystem II
q_P	Photochemical quenching
RCD	Root cortex diameter
RDM	Root dry matter
RMD	Root metaxylem diameter
RDT	Root endodermis thickness
RET	Root epidermis thickness
ROS	Reactive oxygen species
RuBisCO	Ribulose-1,5-bisphosphate carboxylase/oxygenase
SD	Stomatal density
SDM	Stem dry matter
SF	Stomatal functionality
SI	Stomatal index
SOD	Superoxide dismutase
SPT	Spongy parenchyma thickness
TDM	Total dry matter
Total Chl	Total Chlorophyll
VCD	Vascular cylinder diameter
WUE	Water-use efficiency
Φ_{PSII}	Effective quantum yield of PSII photochemistry

1 Introduction

Soybean (*Glycine max* L.) is the most widely cultivated legume around the world due to its high protein and oil content (Singh et al. 2008; Nisa et al. 2016; Baig et al. 2018). Its world production reached 338 million tons in the 2017/2018 harvest, with the United States, Brazil and Argentina being the main producers (FAO 2018). In field conditions, it has been frequently observed that the growth and development of this species can be affected by abiotic stresses induced by nutritional imbalances (Wang et al. 2015; Santos et al. 2017), metal toxicity (Balasaraswathi et al. 2017; Reis et al. 2018), water deficiency (Kunert et al. 2016; Wijewardana et al. 2019), salinity (Shu et al. 2017) and high temperatures (Allen Jr. et al. 2018).

Zinc is the second most necessary micronutrient for plants (Jain et al. 2010), being the deficiency of this element caused by the weathering process in tropical soils (Suhr et al. 2018). On the other hand, the zinc toxicity in plants is mainly determined by the anthropic activity associated to deposition of pollutants rich in heavy metals (Nagajyoti et al. 2010). Many plants contain 3 to 100 μg Zn g^{-1} dry matter, which is considered sufficient to promote adequate plant growth rates, while concentrations above 300 μg Zn g^{-1} are generally considered toxic (Noulas et al. 2018). The Zn content in soil is variable depending on its physical and chemical characteristics, but concentrations higher than 100 μg g^{-1} in soil are unusual (Rezapour et al. 2014; Antoniadis et al. 2018). However, plants frequently exhibit symptoms of Zn deficiency in shoots with concentrations lower than 2 μg Zn g^{-1} dry matter (Sinclair and Krämer 2012).

Zinc is essential for plant growth (Sadeghzadeh 2013; Hafeez et al. 2013) and plays important roles in essential processes, such as membrane biosynthesis, photosynthetic machinery, hormonal regulation, metabolism of lipids and nucleic acids, gene expression, and protein synthesis (Hänsch and Mendel 2009; Noulas et al. 2018; Manaf et al. 2019). Additionally, Zn is the single metal required in all six classes of the enzymes (oxidoreductases, transferases, hydrolases, lyases, isomerases and ligases) essential during photosynthesis processes and subsequent starch accumulation (Palmer and Guerinot 2009; Tripathi et al. 2015).

Deficiency linked to zinc frequently results in lower biomass and yield (Hidoto et al. 2017), reduces chlorophyll levels (Kosesakal and Unal 2009; Samreen et al. 2017) and minor efficiency linked to antioxidant system, more specifically related to superoxide dismutase (SOD) enzyme (Singh et al. 2019). Chloroplast ultrastructure is affected, resulting in abnormalities in leaf structure leading to leaf chlorosis (Kim and Wetzstein 2003; Fu et al. 2015). In relation to the photosynthetic machinery, decreases in the photochemical efficiency and the activities of ribulose-1,5-bisphosphate carboxylase/oxygenase (RuBisCO) and carbonic anhydrase (CA) enzymes have been reported (Salama et al. 2006; Tavallali et al. 2009; Hajiboland and Amirazad 2010). However, excess levels of Zn also promote deleterious effects on crop yield (Tripathi et al. 2015) because Zn toxicity negatively affects CO_2 assimilation and stomatal mechanisms (Azzarello et al. 2012), thus decreasing the transpiration rates and water content in the leaf (Sagardoy et al. 2009) and resulting in a lower biomass (Marques et al. 2017).

The root is a vital organ of the plant and has specialized tissues with important functions connected to influx of water and nutrients (Barberon et al. 2016). The exodermis and endodermis are tissues that act in regard to protection and selectivity of the root, thus contributing to the symplastic immobilization of excesses of Zn in the vacuoles of the root cells (Enstone et al. 2003; Arrivault et al. 2006; Sinclair and Krämer 2012). The cortex is a tissue with a storage capacity for water and nutrients in the root (Hameed et al. 2009). However, under conditions of oxidative stress, reduction and disintegration of cortical cells can occur (Singh et al. 2007; Talukdar 2013), negatively impacting the respiration and nutrient content of the root tissue (Schneider et al. 2017). In plants exposed to low/high availability of nutrients, the cortical tissue can be replaced by the cortical aerenchyma of the root, which allows for a higher allocation of the nutrients to other plant functions, such as growth and reproduction (Fan

et al. 2003; Lynch 2007; Postma and Lynch 2011; Saengwilai et al. 2014).

The exogenous application of 24-epibrassinolide (EBR) can be a possible solution to mitigate the damage caused by deficiencies and excess Zn in plants because EBR is one of the most bioactive forms of brassinosteroids (BRs); it is extracted from plants and is biodegradable (Azhar et al. 2017). This steroid presents a broad spectrum of systemic action on plant metabolism (Oh et al. 2012), including CO_2 (Li et al. 2016b), gas exchange (Swamy and Rao 2009), photochemical efficiency (Thussagunpanit et al. 2015), antioxidant metabolism (Xia et al. 2009) and growth rate (Abdullahi et al. 2003). In addition, BRs activate proton pumps, stimulate the synthesis of proteins and nucleic acids (Bajguz 2000) and modulate cellular expansion and division (Zhiponova et al. 2013).

This study has focused on the gap in the literature in relation to EBR's hypothetical effects in regard to Zn. Zn is the second most common micronutrient required by plants; however, deficiencies and excesses of Zn promote deleterious effects on soybean plants. Interestingly, EBR can be a possible solution to mitigate the damage caused by deficiencies and excesses of Zn in plants because this steroid presents a spectrum of actions linked to increments in nutrient content (Lima et al. 2018), reactive oxygen species scavenging (Oliveira et al. 2019) and stimulation of biomass (Maia et al. 2018). Therefore, the aim of this research was to determine whether EBR can mitigate oxidative stress in soybean plants subjected to different Zn supplies and to evaluate its possible repercussions on anatomical, nutritional, biochemical, physiological and morphological behaviours.

2 Materials and Methods

2.1 Location and Growth Conditions

The experiment was performed at the Campus of Paragominas of the Universidade Federal Rural da Amazônia, Paragominas, Brazil (2°55' S, 47°34' W). The study was conducted in a greenhouse with the temperature and humidity controlled. The minimum, maximum, and median temperatures were 21, 31 and 25.2 °C, respectively. The relative humidity during the experimental period varied between 60% and 80%.

2.2 Plants, Containers and Acclimation

Seeds of *Glycine max* (L.) Merr. var. M8644RR Monsoy™ were germinated and grown in 1.2-L pots filled with a mixed substrate of sand and vermiculite at a ratio of 3:1. The plants were cultivated under semi-hydroponic conditions containing 500 mL of distilled water for eight days. A modified Hoagland and Arnon (1950) solution was used for nutrients, with the ionic strength beginning at 50% (6th day) and later modified to 100% after two days (8th day). After this period, the nutritive solution remained at total ionic strength.

2.3 Experimental Design

The experiment followed a completely randomized factorial design with two concentrations of 24-epibrassinolide (0 and 100 nM EBR, described as - EBR and + EBR, respectively) and three Zn supplies (0.2, 20 and 2000 μM Zn, described as low, control and high supply of Zn). With five replicates for each of six treatments, a total of 30 experimental units were used in the experiment, with one plant in each unit.

2.4 24-Epibrassinolide (EBR) Preparation and Application

Ten-day-old seedlings were sprayed with 24-epibrassinolide (EBR) or Milli-Q water (containing a proportion of ethanol that was equal to that used to prepare the EBR solution) at 5-d intervals until day 35. The 0 and 100 nM EBR (Sigma-Aldrich, USA) solutions were prepared in agreement with Ahammed et al. (2013). Based on preliminary studies and literature available (Lima and Lobato 2017; Maia et al. 2018; Pereira et al. 2019; Oliveira et al. 2019), the EBR is more efficient in plants pretreated (10th day). On the other hand, Zn was applied only on 20th day after experimental implementation due to need of leaf area and plant tissue sufficient to make all analyses involved in this research.

2.5 Plant Conduction and Zn Supplies

The plants received the following macro- and micronutrients contained in the nutrient solution: 8.75 mM KNO_3, 7.5 mM $Ca(NO_3)_2{\cdot}4H_2O$, 3.25 mM $NH_4H_2PO_4$, 1.5 mM $MgSO_4{\cdot}7H_2O$, 62.50 μM KCl, 31.25 μM H_3BO_3, 2.50 μM $MnSO_4{\cdot}H_2O$, 0.63 μM $CuSO_4{\cdot}5H_2O$, 0.63 μM $NaMoO_4{\cdot}5H_2O$ and 250 μM $NaEDTAFe{\cdot}3H_2O$, with Zn concentrations adjusted to each treatment. For Zn treatments, $ZnCl_2$ was used at concentrations of 0.2 μM (low) and 20 μM (control) and 2000 μM (high) applied over 15 days (days 20–35 after the start of the experiment). Plants were maintained from 8th to 20th day under equal Zn concentration (20 μM Zn), considered as control treatment. One plant per pot was used to examine the plant parameters. On day 35 of the experiment, all plants were harvested and analysed.

2.6 Measurement of Chlorophyll Fluorescence and Gas Exchange

The chlorophyll fluorescence was measured in fully expanded leaves under light using a modulated chlorophyll fluorometer (model OS5p; Opti-Sciences). Preliminary tests determined

the location of the leaf, the part of the leaf and the time required to obtain the greatest F_v/fm ratio; therefore, the acropetal third of the leaves, which was the middle third of the plant and adapted to the dark for 30 min, was used in the evaluation. The intensity and duration of the saturation light pulse were 7500 μmol m^{-2} s^{-1} and 0.7 s, respectively. The gas exchange was evaluated in all plants, measuring expanded leaves in middle region of the plant under constant conditions of a CO_2 concentration, using an infrared gas analyser (model LCPro$^+$; ADC BioScientific), photosynthetically active radiation, air-flow rate and temperature in a chamber at 360 μmol mol^{-1} CO_2, 800 μmol photons m^{-2} s^{-1}, 300 μmol s^{-1} and 28 °C, respectively, between 10:00 and 12:00 h. Previous tests using equal soybean variety and greenhouse were conducted to configure the equipment and determinate the work conditions. The water-use efficiency (WUE) was estimated according to Ma et al. (2004), and the instantaneous carboxylation efficiency (P_N/C_i) was calculated using the formula that was described by Aragão et al. (2012).

2.7 Quantifications Linked to Anatomical Variables

Samples were collected from the middle region of the leaf limb of fully expanded leaves and roots 5 cm from the root apex, being used five samples to examine the anatomical variables. Subsequently, all collected botanical material was fixed in FAA 70 for 24 h, dehydrated in ethanol and embedded in historesin Leica™ (Leica, Nussloch, Germany). Transverse sections with a thickness of 5 μm were obtained with a rotating microtome (model Leica RM 2245, Leica Biosystems) and were stained with toluidine blue (O'Brien et al. 1964). For stomatal characterization, the epidermal impression method was used according to Segatto et al. (2004). The slides were observed and photomicrographed under an optical microscope (Motic BA 310, Motic Group Co. LTD.) coupled to a digital camera (Motic 2500, Motic Group Co., LTD.). The images were analysed with Motic plus 2.0, which was previously calibrated with a micrometre slide supplied by the manufacturer. The anatomical parameters evaluated were polar diameter of the stomata (PDS), equatorial diameter of the stomata (EDS), epidermis thickness from adaxial leaf side (ETAd), epidermis thickness from abaxial leaf side (ETAb), palisade parenchyma thickness (PPT), spongy parenchyma thickness (SPT), and the ratio PPT/SPT. In both leaf faces, the stomatal density (SD) was calculated as the number of stomata per unit area and the stomatal functionality (SF) as the ratio PDS/EDS according to Castro et al. (2009). The stomatal index (SI %) was calculated as the percentage of stomata in relation to total epidermal cells by area. In root samples, the root epidermis thickness (RET), root endodermis thickness (RDT), root cortex diameter (RCD), vascular cylinder diameter (VCD) and root metaxylem diameter (RMD) were measured.

2.8 Extraction of Antioxidant Enzymes, Superoxide and Soluble Proteins

Antioxidant enzymes (SOD, CAT, APX and POX), superoxide and soluble proteins were extracted from leaf tissues according to the method of (Badawi et al. 2004). The extraction mixture was prepared by homogenizing 500 mg of fresh plant material in 5 ml of extraction buffer, which consisted of 50 mM phosphate buffer (pH 7.6), 1.0 mM ascorbate and 1.0 mM EDTA. Samples were centrifuged at 14,000×g for 4 min at 3 °C, and the supernatant was collected. Quantification of the total soluble proteins was performed using the method described by (Bradford 1976). Absorbance was measured at 595 nm, using bovine albumin as a standard.

2.9 Superoxide Dismutase Assay

For the SOD assay (EC 1.15.1.1), 2.8 ml of a reaction mixture containing 50 mM phosphate buffer (pH 7.6), 0.1 mM EDTA, 13 mM methionine (pH 7.6), 75 μM NBT, and 4 μM riboflavin was mixed with 0.2 ml of supernatant. The absorbance was then measured at 560 nm (Giannopolitis and Ries 1977).One SOD unit was defined as the amount of enzyme required to inhibit 50% of the NBT photoreduction. The SOD activity was expressed in unit mg^{-1} protein.

2.10 Catalase Assay

For the CAT assay (EC 1.11.1.6), 0.2 ml of supernatant and 1.8 ml of a reaction mixture containing 50 mM phosphate buffer (pH 7.0) and 12.5 mM hydrogen peroxide were mixed, and the absorbance was measured at 240 nm (Havir and McHale 1987). The CAT activity was expressed in μmol H_2O_2 mg^{-1} protein min^{-1}.

2.11 Ascorbate Peroxidase Assay

For the APX assay (EC 1.11.1.11), 1.8 ml of a reaction mixture containing 50 mM phosphate buffer (pH 7.0), 0.5 mM ascorbate, 0.1 mM EDTA, and 1.0 mM hydrogen peroxide was mixed with 0.2 ml of supernatant, and the absorbance was measured at 290 nm (Nakano and Asada 1981). The APX activity was expressed in μmol AsA mg^{-1} protein min^{-1}.

2.12 Peroxidase Assay

For the POX assay (EC 1.11.1.7), 1.78 ml of a reaction mixture containing 50 mM phosphate buffer (pH 7.0) and 0.05% guaiacol was mixed with 0.2 ml of supernatant, followed by addition of 20 μL of 10 mM hydrogen peroxide. The absorbance was then measured at 470 nm (Cakmak and Marschner 1992). The POX activity was expressed in μmol tetraguaiacol mg^{-1} protein min^{-1}.

2.13 Determination of Superoxide Concentration

To determine O_2^-, 1 ml of extract was incubated with 30 mM phosphate buffer [pH 7.6] and 0.51 mM hydroxylamine hydrochloride for 20 min at 25 °C. Then, 17 mM sulphanilamide and 7 mM α-naphthylamine were added to the incubation mixture for 20 min at 25 °C. After the reaction, ethyl ether was added in the identical volume and centrifuged at 3000×g for 5 min. The absorbance was measured at 530 nm (Elstner and Heupel 1976).

2.14 Extraction of Nonenzymatic Compounds

Nonenzymatic compounds (H_2O_2 and MDA) were extracted as described by Wu et al. (2006). Briefly, a mixture for extraction of H_2O_2 and MDA was prepared by homogenizing 500 mg of fresh leaf materials in 5 mL of 5% (*w*/*v*) trichloroacetic acid. Then, the samples were centrifuged at 15,000 x g for 15 min at 3 °C to collect the supernatant.

2.15 Determination of Hydrogen Peroxide Concentration

To measure H_2O_2, 200 μL of supernatant and 1800 μL of reaction mixture (2.5 mM potassium phosphate buffer [pH 7.0] and 500 mM potassium iodide) were mixed, and the absorbance was measured at 390 nm (Velikova et al. 2000).

2.16 Quantification of Malondialdehyde Concentration

MDA was determined by mixing 500 μL of supernatant with 1000 μL of the reaction mixture, which contained 0.5% (*w*/*v*) thiobarbituric acid in 20% trichloroacetic acid. The mixture was incubated in boiling water at 95 °C for 20 min, with the reaction terminated by placing the reaction container in an ice bath. The samples were centrifuged at 10,000×g for 10 min, and the absorbance was measured at 532 nm. The nonspecific absorption at 600 nm was subtracted from the absorbance data. The MDA–TBA complex (red pigment) amount was calculated based on the method of Cakmak and Horst (1991), with minor modifications and using an extinction coefficient of 155 mM^{-1} cm^{-1}.

2.17 Determination of Electrolyte Leakage

Electrolyte leakage was measured according to the method of Gong et al. (1998) with minor modifications. Fresh tissue (200 mg) was cut into pieces 1 cm in length and placed in containers with 8 mL of distilled deionized water. The containers were incubated in a water bath at 40 °C for 30 min, and the initial electrical conductivity of the medium (EC_1) was measured. Then, the samples were boiled at 95 °C for 20 min to release the electrolytes. After cooling, the final electrical conductivity (EC_2) was measured. The percentage of electrolyte leakage was calculated using the formula EL (%) = (EC_1/EC_2) × 100.

2.18 Determination of Photosynthetic Pigments

The chlorophyll and carotenoid determinations were performed with 40 mg of leaf tissue, being used five samples per treatment. The samples were homogenized in the dark with 8 mL of 90% methanol (Nuclear). The homogenate was centrifuged at 6000×g for 10 min at 5 °C. The supernatant was removed, and chlorophyll *a* (Chl *a*) and *b* (Chl *b*), carotenoid (Car) and total chlorophyll (total Chl) contents were quantified using a spectrophotometer (model UV-M51; Bel Photonics), according to the methodology of Lichtenthaler and Buschmann (2001).

2.19 Determination of Nutrients

Samples with 100 mg of milled samples were weighed in 50-mL conical tubes (Falcon^R, Corning, Mexico) and predigested (48 h) with 2 ml of sub boiled HNO_3 (DST 1000, Savillex, USA). After, 8 ml of a solution containing 4 ml of H_2O_2 (30% *v*/v, Synth, Brasil) and 4 ml of ultra-pure water (Milli-Q System, Millipore, USA) were added, and the mixture was transferred to a Teflon digestion vessel, closed and heated in a block digester (EasyDigest®, Analab, France) according to the following program: i) 100 °C for 30 min; ii) 150 °C for 30 min; iii) 130 °C for 10 min; iv) 100 °C for 30 min and; and v) left to cool. The volume was made to 50 mL with ultra-pure water, and iridium was used as an internal standard at 10 μg l^{-1}. The determinations of Zn, P, K, Mg, Fe, Cu and Mo were carried out using an inductively coupled plasma mass spectrometer (ICP-MS 7900, Agilent, USA). Certified reference materials (NIST 1570a and NIST 1577c) were run in each batch for quality control purposes. All found values were in agreement with certified values.

2.20 Measurements of Morphological Parameters

The growth of roots, stems and leaves was measured based on constant dry weights (g) after drying in a forced-air ventilation oven at 65 °C.

2.21 Data Analysis

The data were submitted to ANOVA and applied Scott–Knott test at a probability level of 5% (Steel et al. 2006). All statistical procedures used the Assistat software.

3 Results

3.1 Zn Contents in Plants after EBR and Zn Treatments

The low and high Zn supplies promoted changes in the contents of this element in the root, stem and leaf tissues of soybean plants (Table 1). Plants sprayed with EBR and exposed to low Zn presented increases in Zn concentrations of 48% (root), 42% (stem) and 41% (leaf) when compared to the same treatment without EBR. However, the control + EBR treatment exhibited increases of 44%, 50% and 12% in root, stem and leaf, respectively. In relation to the high Zn with EBR, significant decreases were detected in the Zn contents in the stem and leaf by 21% and 10%, respectively, but there was an increase in the root tissue of 7%.

3.2 Root Structures Were Positively Modulated by EBR

The low and high Zn supplies resulted in negative changes in root anatomy (Fig. 1). However, the application of EBR in the plants submitted to the low Zn treatment promoted increases for RET, RDT, RCD, VCD and RMD of 16%, 3%, 14%, 33% and 74% (Table 2), respectively, when compared to the same treatment without EBR, while the control + EBR treatment had increases of 10%, 5%, 10%, 38% and 5%, respectively. Plants exposed to high Zn + EBR had increases of 25%, 7%, 9% 29% and 69%, respectively.

3.3 EBR Maximized the Nutrient Contents

Soybean plants exposed to low and high concentrations of Zn had reductions ($P < 0.05$) in nutrient contents in their tissues (Table 3). However, plants subjected to a low Zn supply and sprayed with EBR had increases in the values of K, P, Mg, Fe, Cu and Mo at 14%, 15%, 9%, 29%, 23% and 42% (root); 4%, 16%, 15%, 16%, 30% and 12% (stem); 25%, 13%, 12%, 10%, 7% and 55% (leaf), respectively, compared with the same treatment without EBR (Table 3). In the high Zn treatment with EBR, we also observed increases in K, P, Mg, Fe, Cu and Mo of 29%, 13%, 24%, 19%, 37% and 10% in roots; 7%, 12%, 50%, 9%, 9% and 4% in stems; and 6%, 28%, 15%, 17%, 17% and 50% in leaves compared with the equal treatment without EBR.

The steroid provoked benefits for the photosynthetic machinery of plants under Zn stress.

Plants with low and high Zn supplies exhibited reductions in F_m, F_v and F_v/fm, but increase in F_0, in relation control treatment (Fig. 2). In F_m, the EBR application resulted in increases of 2% and 2% in the low and high supplies, respectively, when related to the same treatment without EBR. For F_v, we detected increases of 3% and 3% in plants under low and high Zn supplies with EBR, respectively. In F_v/fm, a low Zn with EBR had an increase of 1%, while the control + EBR showed an increment of 2% in relation to the same treatment without EBR. Decreases in Φ_{PSII}, q_P and ETR and increases in NPQ, EXC and ETR/P_N were verified under low and high Zn in soybean plants (Table 4). However, plants treated with 100 nM EBR and exposed to low Zn had increases of 4%, 4%, and 5% for Φ_{PSII}, q_P and ETR, respectively, and reductions in NPQ (8%) and EXC (1%) compared to the low Zn without EBR. In relation to the high Zn with EBR, there were increases of 16%, 12%, and 14% for Φ_{PSII}, q_P and ETR, respectively, and decreases in NPQ (8%) and EXC (6%) and ETR/P_N (5%) compared with the same treatment in the absence of EBR.

3.4 Exogenous EBR Improved the Gas Exchange

The low and high Zn supplies had negative effects on gas exchange (Table 5). However, the application of EBR in plants with a low Zn supply resulted in increases of P_N, g_s, WUE and P_N/C_i of 5%, 14%, 10% and 32%, respectively, and decreases of 20% for C_i when compared to the same treatment without EBR. The high Zn + EBR had incremental changes in P_N, E, g_s, WUE and P_N/C_i of 20%, 9%, 13%, 10% and 59%, respectively, and a reduction of 19% in C_i.

EBR action enhanced the stomatal performance in plants exposed to different Zn supplies.

The stomatal characteristics showed decreases in SD, SF and SI, as well as increases in PDS and EDS on the adaxial and abaxial faces of soybean leaves exposed to the low and high Zn concentrations (Table 6). The action of EBR on the adaxial face of leaves in both treatments (low and high Zn) caused increases in SD (26% and 76%, respectively), SF (5% and 4%, respectively) and SI (24% and 57%, respectively) and reductions in PDS (4% and 8%, respectively) and EDS (9% and 12%, respectively). For the abaxial face, the low and high Zn supplies with 100 nM EBR spray promoted increases in SD (13% and 30%, respectively), SF (4% and 2%, respectively) and SI (6% and 8%, respectively) and decreases in values of PDS (5% and 8%, respectively) and EDS (10% and 11%, respectively) when compared to the same treatment in the absence of EBR.

Beneficial repercussions on leaf anatomy promoted by the steroids in plants under Zn stress.

The low and high concentrations of Zn promoted negative changes in the leaf anatomy (Fig. 3). However, plants under low Zn and EBR had increases in ETAd (21%), ETAb (25%), PPT (11%) and SPT (12%) and a reduction in PPT/SPT (2%) compared with the same treatment without EBR (Table 7). For the high Zn with EBR, we observed significant increases in ETAd (19%), ETAb (14%), PPT (10%) and SPT (16%) and a decrease in PPT/SPT (6%).

Antioxidant enzymes were stimulated after EBR spray in plants treated with different Zn concentrations.

Table 1 Zn contents in soybean plants sprayed with EBR and exposed to different Zn supplies

EBR	Zn supply	Zn in root (μg g DM^{-1})	Zn in stem (μg g DM^{-1})	Zn in leaf (μg g DM^{-1})
_	Low	8.21 ± 0.19Bb	3.28 ± 0.24Cb	4.33 ± 0.19Cb
_	Control	9.24 ± 0.52Bb	4.65 ± 0.26Bb	9.12 ± 0.20Bb
_	High	2636.76 ± 124.22Aa	342.73 ± 9.02Aa	665.87 ± 6.46Aa
+	Low	12.15 ± 0.93Ba	4.67 ± 0.19Ca	6.10 ± 0.34Ca
+	Control	13.27 ± 0.76Ba	6.96 ± 0.29Ba	10.20 ± 0.33Ba
+	High	2834.10 ± 157.69Aa	270.99 ± 9.77Ab	598.71 ± 7.34Ab

Zn = Zinc. Columns with different uppercase letters between Zn supplies (low, control and high Zn supply under equal EBR level) and lowercase letters between EBR level (with and without EBR under equal Zn supply) indicate significant differences from the Scott-Knott test ($P < 0.05$). Means ± SD, $n = 5$

Soybean plants exposed to low and high Zn supplies had increases ($P < 0.05$) in SOD, CAT, APX and POX values (Fig. 4). The application of 100 nM EBR in plants under a low Zn supply provoked significant increases of 26% 18%, 66% and 25%, respectively, when compared to the low supplement Zn with 0 nM EBR. The high Zn + EBR resulted in significant increases in the activities of SOD (29%), CAT (24%), APX (72%) and POX (44%) compared with the same treatment in the absence of EBR (Fig. 4).

Oxidative stress induced by different Zn supplies was alleviated after treatment with the steroid.

The oxidant compounds (O_2^- and H_2O_2) and indicators of cell damage (MDA and EL) in plants exposed to low and high Zn supplies showed increases (Fig. 5). However, plants with a low supply of Zn and 100 nM EBR had reductions in O_2^- (46%), H_2O_2 (6%), MDA (17%) and EL (10%) levels compared to the low Zn and 0 nM EBR plants. In relation to the high Zn with EBR, decreases were verified in O_2^- (29%), H_2O_2 (2%), MDA (15%) and EL (6%) in comparison with the same treatment in the absence of EBR.

EBR prevented the degradation of photosynthetic pigments in plants under Zn stress.

In both treatments (low and high Zn), a concentration of 100 nM EBR promoted maximization of the photosynthetic pigments (Table 8), increasing the levels of Chl *a* (29% and 31%, respectively), Chl *b* (95% and 65%, respectively), Chl total (38% and 35%, respectively) and Car (38% and 45%, respectively) when compared with equal treatment without EBR (0 nM). In addition, there were reductions in the Chl *a*/Chl *b* ratio of 31% and 14% and in the Chl/Car ratio of 4% and 5%, respectively.

Effects deleterious on the biomass were mitigated in plants treated with EBR and subjected to Zn stress.

Plants under low and high Zn supplies presented improvements in growth when receiving EBR application, for the low Zn + EBR increases of 25%, 32%, 5% and 22% of LDM, RDM, SDM and TDM, respectively, compared to low Zn + 0 nM EBR (Fig. 6). In the high Zn with EBR, we also detected increases in the values of LDM, RDM, SDM and TDM of 14%, 5%, 12% and 10%, respectively.

4 Discussion

Plants exposed to low and control Zn + 100 nM EBR had increases in Zn content, suggesting that this steroid improved the absorption, transport and accumulation of Zn in the evaluated tissues. This result can be associated with the intense interaction between Zn^{2+} ions and organic acids, such as histidine, to form soluble Zn complexes, favouring the absorption and accumulation of this metal in the cytosol of the root cells (Khodamoradi et al. 2015). Histidine is an amino acid that plays a central role in the homeostasis of $^{Zn2+}$ ions, facilitating the mobility of this element in the xylem sap via symplastic transport (Kozhevnikova et al. 2014; Khodamoradi et al. 2015). On the other hand, exogenous EBR also minimized the toxic effects of Zn, reducing the Zn content in the tissues exposed to a high Zn supply. This reduction is related to higher synthesis of phytochelatins (PC) in the root cells (Anwar et al. 2018). PC contributes to detoxification mechanisms of heavy metals (Rajewska et al. 2016), chelating the metal ions and forming complexes, with consequent immobilization of this metal in the cytoplasm of root cells (Bajguz and Hayat 2009; Bajguz 2010). Tadayon and Moafpourian (2019) verified that foliar application of 0.4 mg L^{-1} EBR increased the efficiency of foliar application of Zn and B, affecting the chemical and reproductive characteristics of *Vitis vinifera* plants.

EBR revealed beneficial effects on root tissues (RET, RDT, RCD, VCD and RMD). Increases in the expression of RET, RDT and RCD demonstrated that EBR modulated growth linked to the root meristem through cellular expansion and differentiation, conferring higher protection to this organ (Wei and Li 2016). The epidermis, endoderm and cortex are tissues that are associated with the mechanism of protection and selectivity in the roots, and the increases detected in these tissues contribute to forming a barrier against biotic and abiotic stresses (Cui 2015; Barberon et al. 2016). EBR has positive effects on VCD and RMD, suggesting that the higher densities of these tissues must facilitate transport of water and nutrients via the symplast (Meyer et al. 2011). Reductions in RET and RCD promoted by the high Zn supply

Table 2 Root anatomy in soybean plants sprayed with EBR and exposed to different Zn supplies

EBR	Zn supply	RET (μm)	RDT (μm)	RCD (μm)	VCD (μm)	RMD (μm)
_	Low	11.8 ± 0.6Bb	17.84 ± 0.6Ba	279.7 ± 15.0Bb	250.8 ± 13.0Bb	25.6 ± 1.5Bb
_	Control	13.2 ± 0.6Ab	19.22 ± 0.5Aa	333.9 ± 09.0Ab	282.3 ± 16.0Ab	47.3 ± 2.2Aa
_	High	10.2 ± 0.5Cb	16.82 ± 0.7Ba	252.6 ± 15.2Ba	221.1 ± 14.0Cb	21.8 ± 1.3Cb
+	Low	13.7 ± 0.3Aa	18.43 ± 0.6Ba	319.6 ± 21.2Ba	334.2 ± 12.7Ba	44.6 ± 1.8Ba
+	Control	14.5 ± 0.6Aa	20.20 ± 0.5Aa	366.9 ± 22.5Aa	388.8 ± 31.3Aa	49.5 ± 2.0Aa
+	High	12.8 ± 0.3Ba	17.94 ± 0.7Ba	276.3 ± 16.0Ca	285.3 ± 15.1Ca	36.8 ± 2.2Ca

RET = Root epidermis thickness; RDT = Root endodermis thickness; RCD = Root cortex diameter; VCD = Vascular cylinder diameter; RMD = Root metaxylem diameter. Columns with different uppercase letters between Zn supplies (low, control and high Zn supply under equal EBR level) and lowercase letters between EBR level (with and without EBR under equal Zn supply) indicate significant differences from the Scott-Knott test ($P < 0.05$). Means ± SD, n = 5

(500 μM ZnSO4) were verified by Bazihizina et al. (2014) after studying the impacts of this metal on the cellular structure of *Nicotiana tabacum* roots. Maia et al. (2018) observed in a study with *Solanum lycopersicum* plants that a spray with 100 nM EBR promoted increases in RET (9%), RDT (14%), RCD (12%), VCD (7%) and RMD (17%).

Plants treated with low and high concentrations of Zn and sprayed with 100 nM EBR presented increases in the contents of macronutrients (K, P, and Mg) and micronutrients (Fe, Cu and Mo). The increments induced by the EBR on Zn contents (mainly under low and control Zn supplies) can be explained by the increases in RDM, suggesting higher amounts of root hairs, because this tissue have large contact surface exposed to substrate, facilitating the uptake and mobility of the Zn in plant tissues (Tanaka et al. 2014). These results revealed that the EBR mitigated the negative impacts of Zn on the ionic homeostasis of these essential elements in the absorption channels, optimizing the transport and assimilation process

Table 3 Nutrient contents in soybean plants sprayed with EBR and exposed to different Zn supplies

EBR	Zn supply	K (mg g DM^{-1})	P (mg g DM^{-1})	Mg (mg g DM^{-1})	Fe (μg g DM^{-1})	Cu (μg g DM^{-1})	Mo (μg g DM^{-1})
Contents in root							
_	Low	23.1 ± 0.7Bb	5.9 ± 0.1Bb	5.7 ± 0.2Ab	943.2 ± 28.1Bb	4.84 ± 0.34Cb	2.6 ± 0.2Cb
_	Control	25.7 ± 0.5Ab	9.3 ± 0.3Ab	6.0 ± 0.3Ab	1670.6 ± 36.5Ab	8.92 ± 0.45Ab	4.5 ± 0.2Bb
_	High	23.5 ± 0.8Bb	6.3 ± 0.2Bb	4.5 ± 0.2Bb	864.9 ± 25.3Cb	6.72 ± 0.36Bb	5.0 ± 0.1Ab
+	Low	26.3 ± 0.7Ca	6.8 ± 0.2Ba	6.2 ± 0.1Ba	1215.5 ± 45.9Ba	5.95 ± 0.34Ca	3.7 ± 0.1Ca
+	Control	35.7 ± 1.6Aa	12.7 ± 1.0Aa	6.7 ± 0.1Aa	2333.8 ± 81.9Aa	10.11 ± 0.40Aa	6.0 ± 0.2Aa
+	High	30.2 ± 0.7Ba	7.1 ± 0.3Ba	5.6 ± 0.1Ca	1032.6 ± 42.9Ca	9.22 ± 0.36Ba	5.5 ± 0.1Ba
Contents in stem							
_	Low	26.9 ± 0.9Ba	5.92 ± 0.2Ab	3.4 ± 0.1Bb	58.2 ± 2.1Ab	1.35 ± 0.10Bb	7.7 ± 0.2Cb
_	Control	31.8 ± 1.5Ab	6.12 ± 0.3Ab	3.7 ± 0.1Ab	58.9 ± 2.0Ab	1.69 ± 0.11Ab	9.6 ± 0.1Ab
_	High	16.1 ± 0.7Ca	3.13 ± 0.1Bb	1.2 ± 0.1Cb	23.2 ± 1.8Ba	1.11 ± 0.05Cb	8.9 ± 0.2Ba
+	Low	27.9 ± 1.8Ba	6.85 ± 0.1Aa	3.9 ± 0.2Aa	67.3 ± 3.0Aa	1.75 ± 0.07Ba	8.6 ± 0.1Ca
+	Control	39.0 ± 0.4Aa	7.05 ± 0.3Aa	4.2 ± 0.2Aa	69.4 ± 0.9Aa	1.98 ± 0.08Aa	10.7 ± 0.3Aa
+	High	17.3 ± 1.7Ca	3.50 ± 0.1Ba	1.8 ± 0.1Ba	25.4 ± 1.5Ba	1.21 ± 0.03Ca	9.3 ± 0.3Ba
Contents in leaf							
_	Low	17.4 ± 0.1Bb	7.1 ± 0.1Bb	4.1 ± 0.1Bb	77.6 ± 1.2Bb	1.22 ± 0.02Bb	3.1 ± 0.1Cb
_	Control	18.6 ± 0.2Aa	7.7 ± 0.1Ab	4.4 ± 0.1Ab	114.7 ± 1.6Ab	1.43 ± 0.05Ab	4.3 ± 0.1Ab
_	High	14.1 ± 0.5Ca	2.9 ± 0.1Cb	3.3 ± 0.1Cb	52.0 ± 0.9Cb	1.16 ± 0.01Cb	3.6 ± 0.1Bb
+	Low	21.7 ± 0.6Aa	8.0 ± 0.1Ba	4.6 ± 0.1Ba	85.5 ± 2.4Ba	1.31 ± 0.04Ba	4.8 ± 0.1Ca
+	Control	19.3 ± 0.9Ba	8.5 ± 0.1Aa	4.8 ± 0.0Aa	127.6 ± 0.2Aa	1.69 ± 0.04Aa	6.1 ± 0.2Aa
+	High	15.0 ± 0.9Ca	3.7 ± 0.1Ca	3.8 ± 0.1Ca	61.0 ± 3.7Ca	1.36 ± 0.05Ba	5.4 ± 0.1Ba

Mg = Magnesium; P = Phosphorus; K = Potassium; Fe = Iron; Cu = Copper; Mo = Molybdenum. Columns with different uppercase letters between Zn supplies (low, control and high Zn supply under equal EBR level) and lowercase letters between EBR level (with and without EBR under equal Zn supply) indicate significant differences from the Scott-Knott test ($P < 0.05$). Means ± SD, n = 5

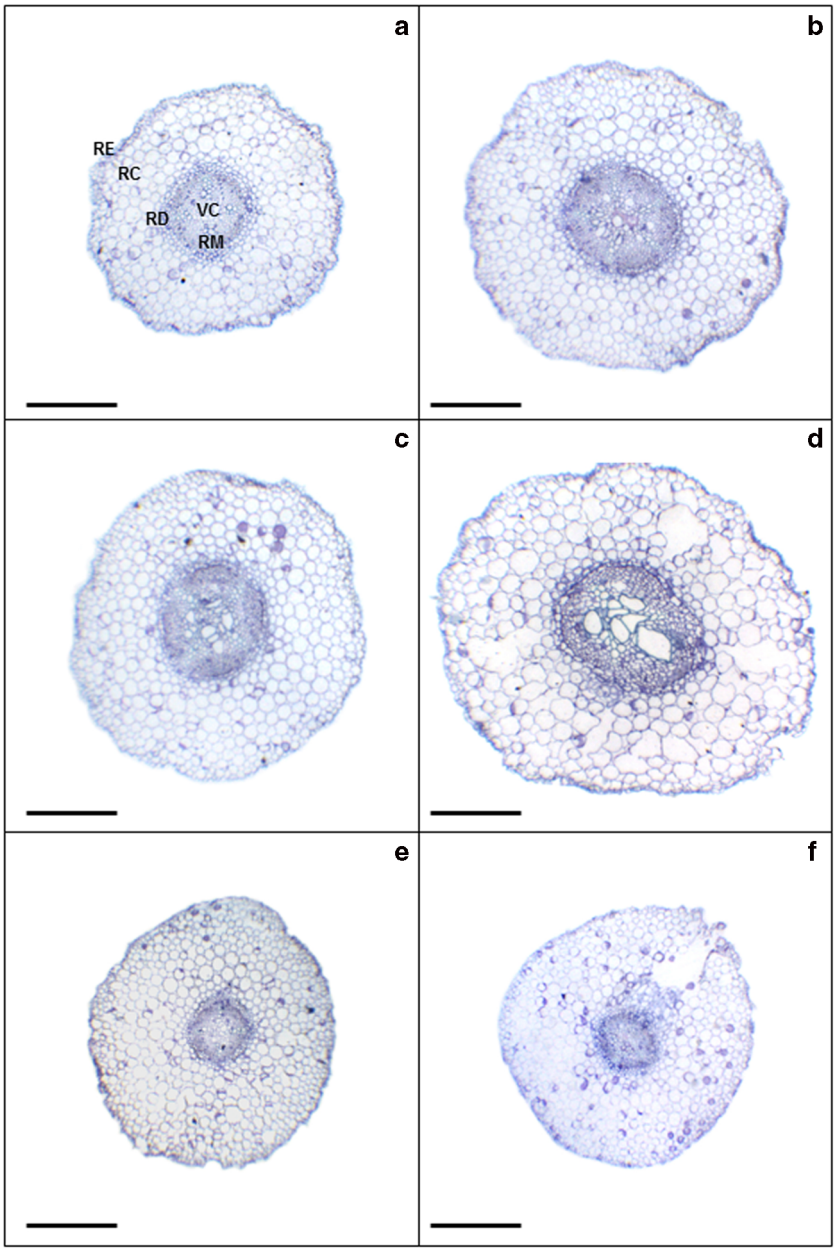

Fig. 1 Root cross sections in soybean plants sprayed with EBR and exposed to different Zn supplies. Low Zn without EBR (A), Low Zn with EBR (B), Control Zn without EBR (C), Control Zn with EBR (D), High Zn without EBR (E), High Zn with EBR (F). RE = Root epidermis; RC = Root cortex; RD = Root endodermis; VC = Vascular cylinder; RM = Root metaxylem. Bars: 300 μm

of $H_2PO_4^-$, Ca^{2+}, Mg^{2+}, Mn^{2+} Fe^{3+}, Cu^{2+} and Zn^{2+} ions by the roots (Karlidag et al. 2011). The exogenous steroid increased the uptake of the Mg^{2+} ion in the root and improved the transport of this element from root to shoot, increasing the chlorophyll levels and improving the photosynthetic characteristics (Fiedor et al. 2008; Yuan et al. 2015). In addition, increases in Fe, Cu, Zn and Mn contribute to a better response related to the antioxidant system because they are metal cofactors of the three main forms of SOD (Fe-SOD, Cu / Zn-SOD and Mn-SOD) (Hänsch and Mendel 2009; Abreu and Cabelli 2010). A study conducted by Samreen et al. (2017) evaluating the effect of Zn stress (0, 1 and 2 μM Zn) on the growth, chlorophyll content and mineral content of *Vigna radiata* plants verified that Zn toxicity had deleterious effects on P, K, and Fe contents in plants. Billard et al. (2015) investigated the impacts of Zn deficiency on nutritional status and protein modifications in *Brassica napus* plants and found that Zn-deficient plants exhibited a lower absorption of elements (K, Mg and Fe).

The exogenous application of 100 nM EBR mitigated the negative effects of low and high Zn supplies on F_0, F_m, F_v and F_v/fm, indicating that EBR reduced photoinhibition and improved photochemical efficiency. Reductions in F_0 and increases in F_m suggested that EBR enhanced the electron transfer from the primary plastoquinone acceptor (Q_A) to the secondary plastoquinone acceptor (Q_B) on the acceptor side of PSII, reflecting positively on F_v/fm (Shu et al. 2016). Andrejić et al. (2018), studying the impact of Zn excess (250, 500 and

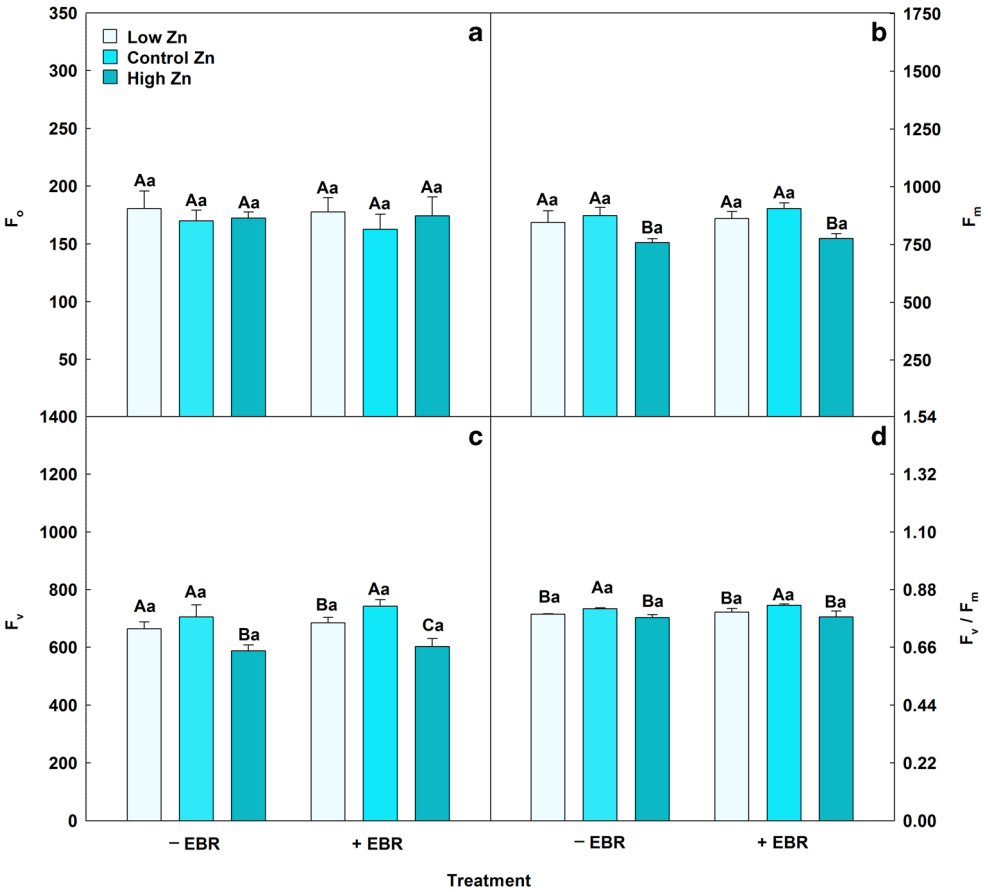

Fig. 2 Minimal fluorescence yield of the dark-adapted state (F_0), maximal fluorescence yield of the dark-adapted state (F_m), variable fluorescence (F_v) and maximal quantum yield of PSII photochemistry (F_v/fm) in soybean plants sprayed with EBR and exposed to different Zn supplies. Columns with different letters indicate significant differences from the Scott-Knott test ($P < 0.05$). Columns corresponding to means from five repetitions and standard deviations

1000 mg Zn kg-1) on gas exchange and chlorophyll fluorescence in plants *Miscanthus* × *giganteus*, verified reductions in F_m, F_v and F_v/fm, while Xia et al. (2009) confirmed in a study with *Cucumis sativus* that 0.1 μM EBR increased the F_v/fm values, optimizing the activity of PSII.

The highest values of Φ_{PSII}, q_p and ETR are intrinsically related to the increase in F_v/fm, as previously described in this study. These results confirm that exogenous EBR maximized the energy capture efficiency by the PSII open-reaction centres in Zn-stressed plants (Zhang et al. 2013; Jia et al. 2015). In addition, the increase in ETR, as indicated by higher values of $\Phi_{PSII,}$ corroborates that EBR increased the capacity of the photosynthetic apparatus to maintain the Q_A in the oxidized state, optimizing the transport of electrons through PSII (Dobrikova et al. 2014). Siddiqui et al. (2018), investigating the chlorophyll fluorescence of *Brassica juncea* plants pretreated with two BRs, detected increases promoted by EBR (10^{-8} M) in Φ_{PSII} (19%), q_p (17%) and ETR (19%), while

Table 4 Chlorophyll fluorescence in soybean plants sprayed with EBR and exposed to different Zn supplies

EBR	Zn supply	Φ_{PSII}	q_P	NPQ	ETR (μmol m^{-2} s^{-1})	EXC (μmol m^{-2} s^{-1})	ETR/P_N
_	Low	0.26 ± 0.02Aa	0.69 ± 0.03Ba	0.96 ± 0.02Aa	38.2 ± 3.5Aa	0.67 ± 0.04Aa	2.49 ± 0.22Aa
_	Control	0.28 ± 0.01Ab	0.80 ± 0.02Aa	0.68 ± 0.02Ca	40.4 ± 2.3Ab	0.66 ± 0.01Aa	2.36 ± 0.22Aa
_	High	0.25 ± 0.01Ab	0.68 ± 0.01Bb	0.75 ± 0.01Ba	36.9 ± 2.3Ab	0.67 ± 0.01Aa	2.61 ± 0.16Aa
+	Low	0.27 ± 0.03Ba	0.72 ± 0.04Ba	0.88 ± 0.02Ab	40.0 ± 3.5Ba	0.66 ± 0.01Aa	2.50 ± 0.08Aa
+	Control	0.32 ± 0.01Aa	0.84 ± 0.03Aa	0.61 ± 0.02Cb	47.3 ± 2.0Aa	0.61 ± 0.02Bb	2.35 ± 0.16Aa
+	High	0.29 ± 0.01Ba	0.76 ± 0.01Ba	0.69 ± 0.01Bb	42.1 ± 1.7Ba	0.63 ± 0.01Bb	2.48 ± 0.11Aa

Φ_{PSII} = Effective quantum yield of PSII photochemistry; q_P = Photochemical quenching coefficient; NPQ = Nonphotochemical quenching; ETR = Electron transport rate; EXC = Relative energy excess at the PSII level; ETR/P_N = Ratio between the electron transport rate and net photosynthetic rate. Columns with different uppercase letters between Zn supplies (low, control and high Zn supply under equal EBR level) and lowercase letters between EBR level (with and without EBR under equal Zn supply) indicate significant differences from the Scott-Knott test ($P < 0.05$). Means ± SD, n = 5

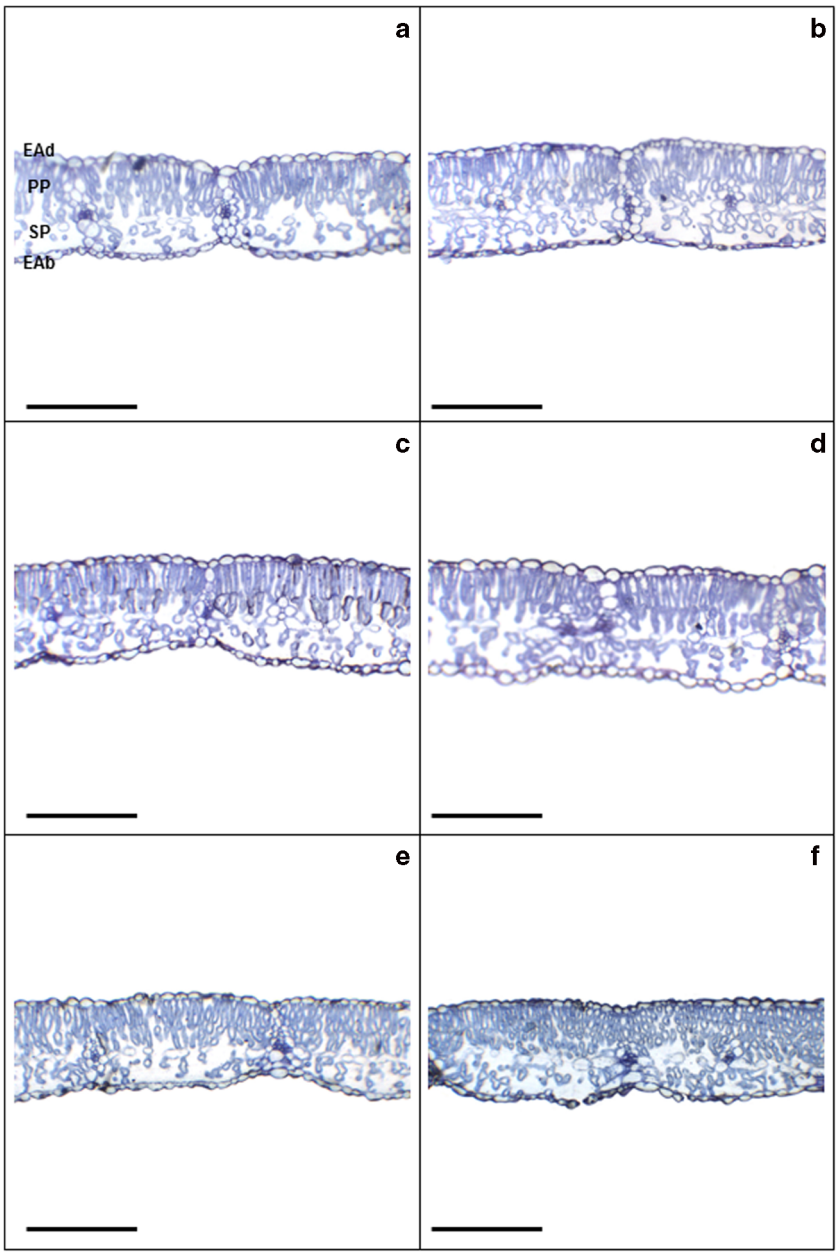

Fig. 3 Leaf cross sections in soybean plants sprayed with EBR and exposed to different Zn supplies. Low Zn without EBR (A), Low Zn with EBR (B), Control Zn without EBR (C), Control Zn with EBR (D), High Zn without EBR (E), High Zn with EBR (F). EAd = adaxial epidermis; EAb = Abaxial epidermis; PP = Palisade parenchyma; SP = Spongy parenchyma. Bars: 200 μm

Table 5 Gas exchange in soybean plants sprayed with EBR and exposed to different Zn supplies

EBR	Zn supply	P_N (μmol m^{-2} s^{-1})	E (mmol m^{-2} s^{-1})	g_s (mol m^{-2} s^{-1})	C_i (μmol mol^{-1})	WUE (μmol$mmol^{-1}$)	P_N/C_i (μmol m^{-2} s^{-1} Pa^{-1})
_	Low	15.4 ± 0.8Ba	2.88 ± 0.10Aa	0.21 ± 0.02Ba	302 ± 12Ba	5.38 ± 0.43Ab	0.056 ± 0.002Bb
_	Control	17.3 ± 0.7Ab	3.02 ± 0.11Aa	0.39 ± 0.01Aa	270 ± 14Ca	5.73 ± 0.32Ab	0.065 ± 0.003Ab
_	High	14.2 ± 0.9Bb	2.63 ± 0.06Bb	0.23 ± 0.02Ba	338 ± 13Aa	5.40 ± 0.20Ab	0.041 ± 0.002Cb
+	Low	16.2 ± 1.5Ba	2.75 ± 0.11Ba	0.24 ± 0.02Ba	243 ± 13Ab	5.91 ± 0.18Ba	0.074 ± 0.003Ba
+	Control	20.2 ± 1.2Aa	3.08 ± 0.04Aa	0.39 ± 0.01Aa	252 ± 21Aa	6.58 ± 0.19Aa	0.089 ± 0.006Aa
+	High	17.1 ± 1.4Ba	2.87 ± 0.07Ba	0.26 ± 0.02Ba	273 ± 19Ab	5.95 ± 0.20Ba	0.065 ± 0.002Ca

P_N = Net photosynthetic rate; E = Transpiration rate; g_s = Stomatal conductance; C_i = Intercellular CO_2 concentration; WUE = Water-use efficiency; P_N/C_i = Carboxylation instantaneous efficiency. Columns with different uppercase letters between Zn supplies (low, control and high Zn supply under equal EBR level) and lowercase letters between EBR level (with and without EBR under equal Zn supply) indicate significant differences from the Scott-Knott test ($P < 0.05$). Means ± SD, n = 5

Table 6 Stomatal characteristics in soybean plants sprayed with EBR and exposed to different Zn supplies

EBR	Zn supply	SD (stomata per mm^2)	PDS (μm)	EDS (μm)	SF	SI (%)
Adaxial face						
_	Low	178 ± 6Bb	13.4 ± 0.3Ba	23.5 ± 0.9Ba	0.57 ± 0.01Ba	7.5 ± 0.6Bb
_	Control	242 ± 3Ab	12.9 ± 0.8Ba	21.3 ± 0.8Ca	0.61 ± 0.01Aa	9.7 ± 0.4Ab
_	High	85 ± 7Cb	14.4 ± 0.2Aa	25.8 ± 0.6Aa	0.56 ± 0.03Ba	4.7 ± 0.3Cb
+	Low	225 ± 9Ba	12.8 ± 0.9Aa	21.4 ± 0.5Bb	0.60 ± 0.05Aa	9.3 ± 0.5Ba
+	Control	250 ± 2Aa	12.3 ± 0.5Aa	20.2 ± 1.5Ba	0.61 ± 0.03Aa	10.7 ± 0.2Aa
+	High	150 ± 8Ca	13.2 ± 0.4Ab	22.8 ± 0.2Ab	0.58 ± 0.04Aa	7.4 ± 0.3Ca
Abaxial face						
_	Low	357 ± 2Bb	13.2 ± 0.4Ba	24.1 ± 0.8Ba	0.55 ± 0.04Aa	34.3 ± 0.8Bb
_	Control	427 ± 8Ab	12.2 ± 0.3Ca	21.6 ± 1.0Ca	0.57 ± 0.04Aa	36.5 ± 0.6Ab
_	High	257 ± 8Cb	14.3 ± 0.2Aa	26.8 ± 0.9Aa	0.54 ± 0.04Aa	33.1 ± 0.9Bb
+	Low	404 ± 9Ba	12.5 ± 0.3Aa	21.8 ± 0.7Bb	0.57 ± 0.04Aa	36.5 ± 0.7Ba
+	Control	457 ± 7Aa	11.2 ± 0.4Bb	18.8 ± 1.2Cb	0.60 ± 0.05Aa	38.8 ± 0.4Aa
+	High	335 ± 6Ca	13.1 ± 0.6Ab	23.9 ± 0.5Ab	0.55 ± 0.04Aa	35.9 ± 0.8Ba

SD = Stomatal density; PDS = Polar diameter of the stomata; EDS = Equatorial diameter of the stomata; SF = Stomatal functionality; SI = Stomatal index. Columns with different uppercase letters between Zn supplies (low, control and high Zn supply under equal EBR level) and lowercase letters between EBR level (with and without EBR under equal Zn supply) indicate significant differences from the Scott-Knott test ($P < 0.05$). Means ± SD, n = 5

foliar spray of HBL (10^{-8} M) promoted increases of 17%, 16% and 18% for Φ_{PSII}, q_p and ETR, respectively.

The decrease induced by EBR in the NPQ, EXC and ETR/P_N of plants exposed to the low and high Zn supplies revealed that the application of this steroid resulted in less excitation energy dissipation in the form of heat, avoiding the damage by photoinhibition in the centres of reaction (Ogweno et al. 2008; Zhang et al. 2015). Additionally, reductions of the expression of EXC and ETR/P_N indicated that the excess electrons were used less often for secondary processes, such as photorespiration, and thus were potentially available for primary processes, such as reductions of $NADP^+$ during the biochemical fixation of CO_2 (Silva et al. 2012). Lima et al. (2018) found that the application of 100 nM EBR in *Eucalyptus urophylla* under Fe deficiency significantly reduced the values of NPQ (19%), EXC (14%) and ETR/P_N (16%), promoting protection of PSII against possible damages caused by the excess of excitation and improving the use of electrons during the photochemical activity.

EBR minimized the damage caused by Zn concentrations (low and high) on gas exchange. Increases in P_N and E are positively related to the improvements expressed in g_s, and these effects are explained by the positive impact of EBR on the enzymatic activities of CA (Hayat et al. 2011) and RuBisCO (Yu et al. 2004), which are key enzymes in the initial process of photosynthesis. The high CA activity increases the carboxylation state of RuBisCO in the Calvin cycle, consequently decreasing C_i and inducing P_N maximization (Hasan et al. 2011; Alyemeni and Al-Quwaiz 2016). The increase in WUE is associated with the benefits promoted by EBR on P_N. In addition, P_N/C_i values were increased in EBR-treated plants due to

Table 7 Leaf anatomy in soybean plants sprayed with EBR and exposed to different Zn supplies

EBR	Zn supply	ETAd (μm)	ETAb (μm)	PPT (μm)	SPT (μm)	Ratio PPT/SPT
_	Low	15.6 ± 1.3Bb	14.2 ± 0.2Bb	84.4 ± 2.0Bb	77.6 ± 3.2Bb	1.09 ± 0.03Ba
_	Control	18.5 ± 0.7Aa	17.4 ± 0.2Ab	93.3 ± 5.0Aa	88.0 ± 4.0Aa	1.06 ± 0.01Ba
_	High	14.9 ± 1.0Bb	13.8 ± 0.9Bb	76.8 ± 3.0Cb	65.4 ± 4.7Cb	1.18 ± 0.01Aa
+	Low	18.8 ± 0.6Aa	17.7 ± 0.7Aa	93.6 ± 2.4Aa	87.2 ± 1.7Aa	1.07 ± 0.03Aa
+	Control	18.9 ± 1.3Aa	18.9 ± 0.5Aa	95.5 ± 5.4Aa	91.8 ± 4.1Aa	1.04 ± 0.03Aa
+	High	17.8 ± 0.7Aa	15.8 ± 0.4Ba	84.1 ± 3.5Ba	75.8 ± 3.9Ba	1.11 ± 0.01Ab

ETAd = Epidermis thickness from adaxial leaf side; ETAb = Epidermis thickness from abaxial leaf side; PPT = Palisade parenchyma thickness; SPT = Spongy parenchyma thickness. Columns with different uppercase letters between Zn supplies (low, control and high Zn supply under equal EBR level) and lowercase letters between EBR level (with and without EBR under equal Zn supply) indicate significant differences from the Scott-Knott test ($P < 0.05$). Means ± SD, n = 5

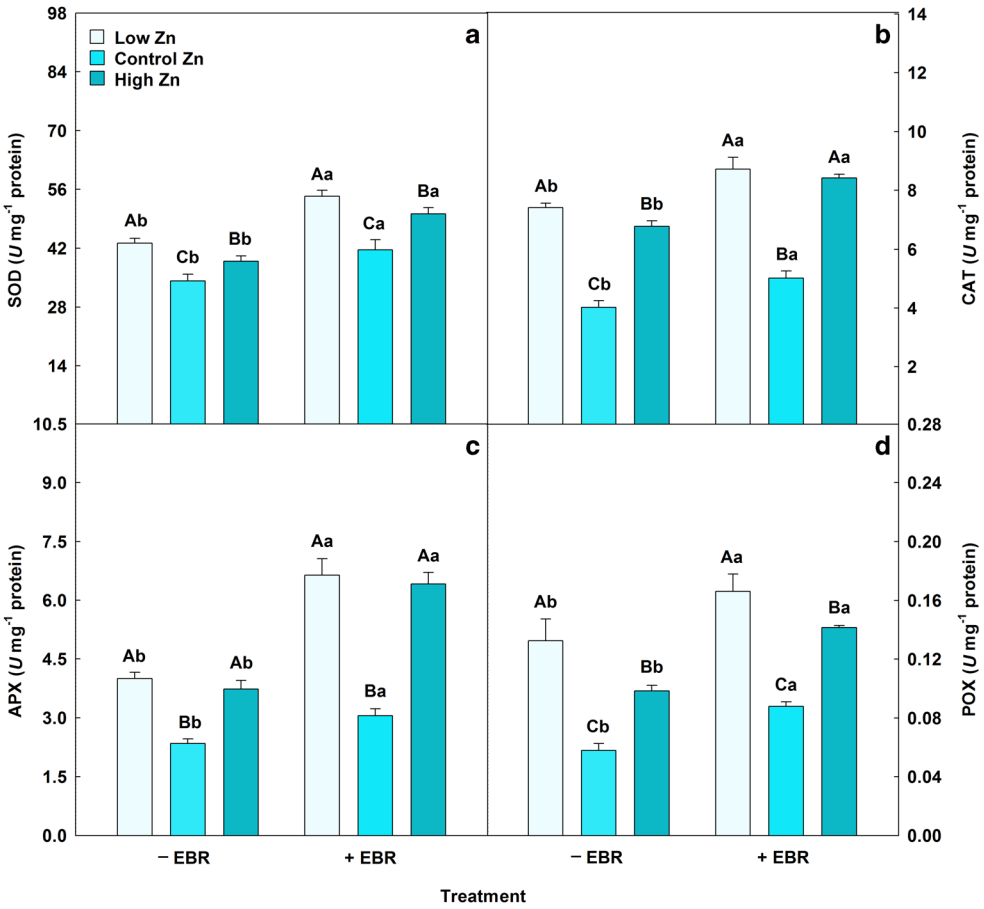

Fig. 4 Activities of superoxide dismutase (SOD), catalase (CAT), ascorbate peroxidase (APX) and peroxidase (POX) in soybean plants sprayed with EBR and exposed to different Zn supplies. Columns with different letters indicate significant differences from the Scott-Knott test ($P < 0.05$). Columns corresponding to means from five repetitions and standard deviations

increased P_N and a simultaneous reduction in C_i. Fei et al. (2016) detected reductions in P_N, g_s and E, as well as increases in C_i promoted by the low Zn supplement in *Citrus sinensis* plants. Ouni et al. (2016), analysing the effects of Zn concentrations (100 and 300 ppm) on the gas exchange of *Polypogon monspeliensis*, observed reductions in P_N, g_s and WUE values under the highest concentration of Zn (300 ppm). However, Jiang et al. (2012) demonstrated that the effects of EBR foliar spraying (0.1 μM) improved the gas exchange (P_N, g_s and C_i) in *Cucumis sativus* plants.

Exogenous EBR (100 nM) had positive effects on stomatal characteristics (SD, PDS, EDS, SF and SI). The increases of SD, SF and SI revealed that the EBR improved stomatal performance, corroborated by higher values detected for g_s. This steroid regulates stomatal development, activating specific proteins that act on the stomatal intracellular signalling pathway (Kim et al. 2012; Casson and Hetherington 2012), maximizing the gas exchange and increasing the opportunity for CO_2 uptake by the mesophyll cells (PPT and SPT) (Flexas et al. 2008, 2012). Additionally, the reductions observed in PDS and EDS reveal beneficial interferences of the EBR in the stomata form, inducing stomata to be more elliptic and providing increases in SF (Martins et al. 2015). Subba et al. (2014), investigating physiological and biochemical changes induced by nine concentrations of Zn (0–20 mM Zn) in *Citrus reticulata* seedlings, observed reductions in SD in the leaves of plants exposed to deficiency (0, 1, 2, 3 and 4 mM Zn) and excess (10, 15 and 20 mM Zn) when compared to a sufficient concentration (5 mM Zn).

Plants treated with EBR (100 nM) and exposed to Zn supplies (low and high) had beneficial effects on leaf anatomy (ETAd, ETAb, PPT and SPT). The increases in PPT and SPT are connected to increments shown in P_N and P_N/C_i because the gas exchange has an influence on the mesophyll, facilitating CO_2 diffusion from the environment to the carboxylation sites in the chloroplasts (Ennajeh et al. 2010). The high values of ETAd and ETAb in plants sprayed with EBR can be explained by the higher values of E and WUE, in which the epidermis is a coating tissue, clearly contributing to the use of water and avoiding excessive loss of water during the transpiration process (Javelle et al. 2011). Kim and Wetzstein (2003) investigated *Carya illinoinensis* plants subjected to Zn deficiency and reported decreases in PPT and SPT

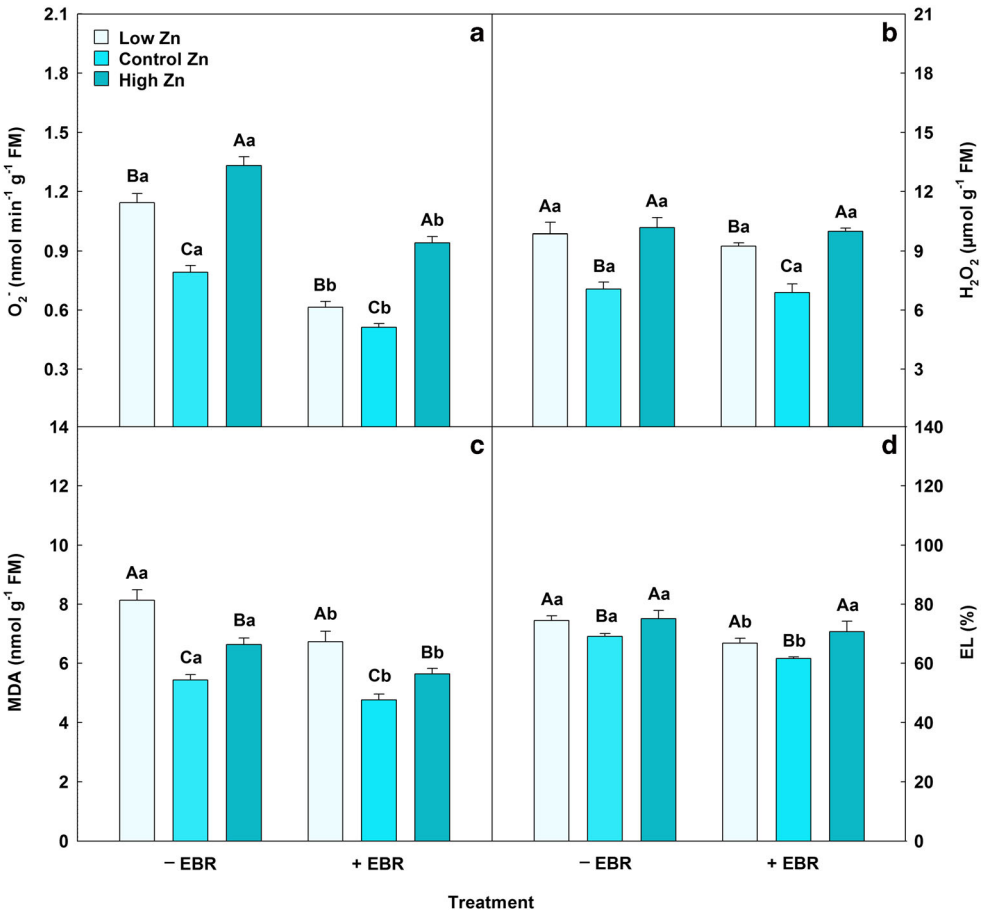

Fig. 5 Superoxide (O_2^-), hydrogen peroxide (H_2O_2), malondialdehyde (MDA) and electrolyte leakage (EL) in soybean plants sprayed with EBR and exposed to different Zn supplies. Columns with different letters indicate significant differences from the Scott-Knott test ($P < 0.05$). Columns corresponding to means from five repetitions and standard deviations

and found a reduction in the number of cells of the palisade parenchyma per length in leaf. Mattiello et al. (2015) examined the impacts of Zn deficiency on physiological and anatomical characteristics of *Zea mays* leaves during 0, 2, 6, 10, 14, 18 and 22 days after the Zn omission; they reported intense reductions in their size, composed of 44% mesophyll and 8% intercellular space. In addition, the epidermal area on the adaxial and abaxial surfaces corresponded to 15% and 10%, respectively.

The application of EBR (100 nM) contributed to an increase in the activities of the SOD, CAT, APX and POX enzymes of the plants exposed to the low and high Zn supplies, revealing the intrinsic action of this substance on antioxidant metabolism. These changes contribute to a higher photochemical efficiency, as evidenced by the increases in F_v/fm and ETR. A study conducted by He et al. (2016) evaluating the enzymatic responses and growth of *Solanum melongena* seedlings

Table 8 Photosynthetic pigments in soybean plants sprayed with EBR and exposed to different Zn supplies

EBR	Zn supply	Chl *a* (mg g^{-1} FM)	Chl *b* (mg g^{-1} FM)	Total Chl (mg g^{-1} FM)	Car (mg g^{-1} FM)	Ratio Chl *a*/Chl *b*	Ratio Total Chl/Car
_	Low	8.19 ± 0.36Bb	1.37 ± 0.05Bb	9.56 ± 0.31Bb	0.48 ± 0.01Bb	6.06 ± 0.41Aa	20.88 ± 0.50Aa
_	Control	12.38 ± 1.12Aa	3.04 ± 0.06Ab	15.42 ± 0.83Aa	0.84 ± 0.02Ab	4.33 ± 0.10Ba	19.60 ± 0.24Ba
_	High	7.41 ± 0.50Bb	1.17 ± 0.04Cb	8.59 ± 0.19Cb	0.42 ± 0.01Cb	6.36 ± 0.41Aa	21.07 ± 0.60Aa
+	Low	10.53 ± 0.30Ba	2.67 ± 0.14Ba	13.20 ± 0.57Ba	0.66 ± 0.02Ba	4.20 ± 0.24Bb	19.96 ± 0.54Aa
+	Control	12.45 ± 0.44Aa	3.21 ± 0.08Aa	15.67 ± 1.10Aa	0.91 ± 0.02Aa	3.95 ± 0.15Ba	18.15 ± 0.44Bb
+	High	9.69 ± 0.20Ca	1.93 ± 0.15Ca	11.62 ± 0.39Ca	0.61 ± 0.01Ca	5.46 ± 0.33Ab	20.04 ± 0.49Aa

Chl *a* = Chlorophyll *a*; Chl *b* = Chlorophyll *b*; Total chl = Total chlorophyll; Car = Carotenoids. Columns with different uppercase letters between Zn supplies (low, control and high Zn supply under equal EBR level) and lowercase letters between EBR level (with and without EBR under equal Zn supply) indicate significant differences from the Scott-Knott test ($P < 0.05$). Means ± SD, n = 5

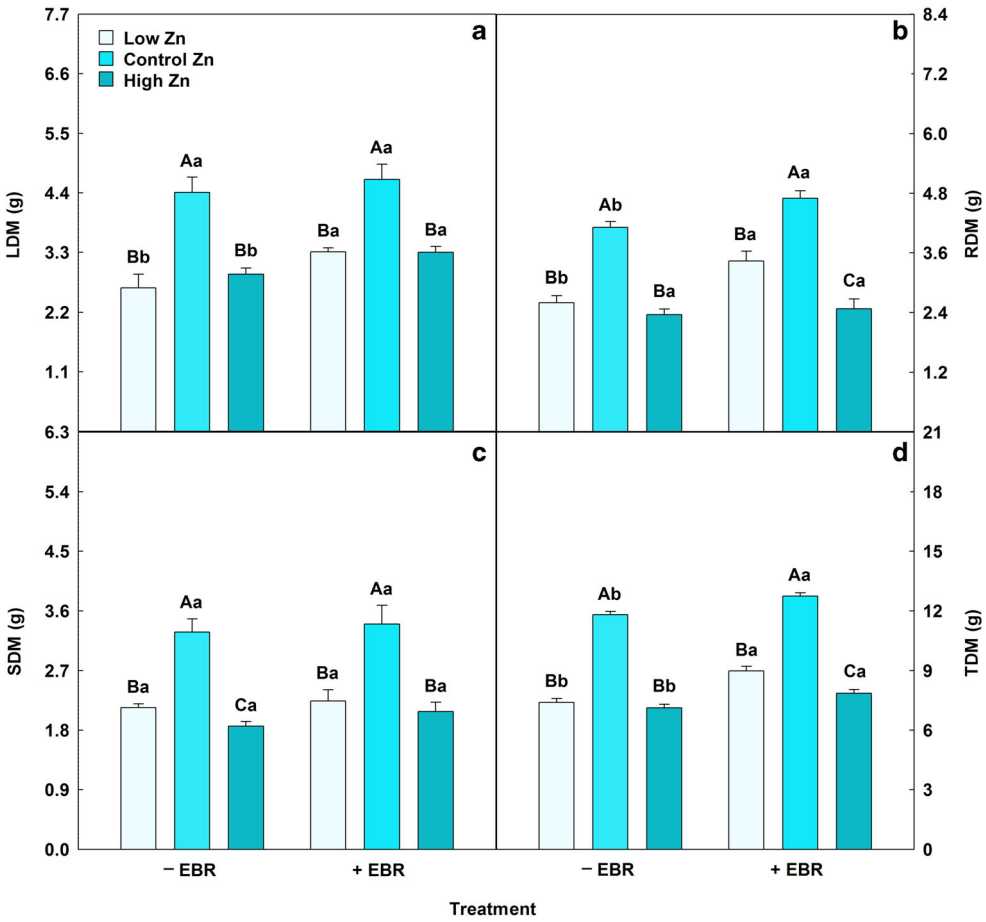

Fig. 6 Leaf dry matter (LDM), root dry matter (RDM), stem dry matter (SDM) and total dry matter (TDM) in soybean plants sprayed with EBR and exposed to different Zn supplies. Columns with different letters indicate significant differences from the Scott-Knott test ($P < 0.05$). Columns corresponding to means from five repetitions and standard deviations

subjected to Zn toxicity (10% Zn) + 0.1 μM EBR detected increases in the activities of SOD (20%), CAT (25%), APX (11%) and POX (17%). Li et al. (2016a), investigating the exogenous effects of EBR on *Solanum lycopersicum* seedlings, also found benefits on the antioxidant system, in which 5 nM EBR notably increased the activities of the SOD, CAT and APX enzymes under Zn stress.

Exogenous EBR (100 nM) promoted reductions in ROS levels (O_2^- and H_2O_2) and mitigated the membrane damage (MDA and EL) in *Glycine max* plants exposed to Zn stress (low and high), and these results were attributed to higher activity of the antioxidant enzymes (SOD, CAT, APX and POX) as previously detected in this study. In cells, the SOD enzyme rapidly converts O_2^- to H_2O_2, while the CAT and APX enzymes act to dissociate H_2O_2, with consequent formation of H_2O and O_2, reducing the concentrations of oxidizing compounds (Li et al. 2016a). On the other hand, high concentrations of O_2^- and H_2O_2 often promote lipid peroxidation (MDA), inducing electrolyte leakage (EL) and negatively impacting the membrane function (Kumari et al. 2010; Gallego et al. 2012). Ramakrishna and Rao (2012) evaluated *Raphanus sativus* seedlings subjected to three concentrations of EBR (0.5, 1.0 and 2 μM) and exposed to Zn stress and verified significant reductions in O_2^- (57%), H_2O_2 (27%) and EL.

Plants under Zn stress (low and high) and sprayed with EBR had increases in the levels of Chl *a*, Chl *b*, Chl total and Car, and these effects were related to lower accumulation of ROS (O_2^- and H_2O_2) in leaf tissue, reducing the oxidative damage to the structures and functions of the thylakoid membranes (Ramakrishna and Rao 2012). This result was confirmed by the decreases in the MDA and EL levels previously described in this study. In addition, EBR promoted an increase in Mg content, which is a structural element of the chlorophyll molecule (Fiedor et al. 2008). These benefits induced by EBR enhanced pigment biosynthesis and promoted a positive impact on the photosynthetic apparatus. Mateos-Naranjo et al. (2018) found reductions in Chl *a*, Chl *b* and Car levels in *Juncus acutus* plants exposed to Zn toxicity (100 mM Zn). However, Ramakrishna and Rao (2015) demonstrated that foliar application of EBL and HBL at concentrations of 0.5, 1.0 and 2.0 μM effectively alleviated the deleterious effects of Zn toxicity on *Raphanus sativus*, protecting mainly the chloroplast membranes and increasing Chl *a*, Chl *b* and Car.

The EBR application reduced the deleterious effects on plant biomass (LDM, RDM, SDM and TDM) caused by low and high Zn supplementation. These results suggest

that EBR stimulated cell division and elongation in roots, stems and leaves, increasing the rate of growth and development (Müssig 2005; Que. et al. 2018). The increase in biomass can be explained by the benefits to root anatomy, gas exchange, antioxidant enzymes (SOD, CAT, APX and POX) and nutrient contents demonstrated in this study (Shahbaz et al. 2008; Hayat et al. 2012; Santos et al. 2018). Pascual et al. (2016) reported significant reductions in the LDM and RDM values of *Glycine max* plants subjected to Zn deficiency. Research conducted by Marques et al. (2017) studying *Jatropha curcas* plants subjected to different concentrations of Zn (100, 200, 300, 400 and 600 μM) observed a decrease in plant biomass (leaf, stem and root) after exposure to a higher concentration of Zn (600 μM).

5 Conclusion

Our study proved that 24-epibrassinolide mitigated the oxidative stress induced by different zinc supplies in soybean plants. In other hand, plants exposed to high zinc supply without 24-epibrassinolide application presented deleterious effects more intense. The steroid spray alleviated the impact produced by zinc stress on nutritional status because these results were intrinsically linked to improvements on vascular cylinder and metaxylem, improving the magnesium, phosphorus, potassium, iron, copper and molybdenum contents. In relation to the photosynthetic machinery of plants treated with 24-epibrassinolide and exposed to high and low zinc supplies, antioxidant enzymes play crucial roles, dismutating superoxide and hydrogen peroxide, and protecting the chloroplast membranes, with clear positive repercussions on chlorophylls, effective quantum yield of photosystem II photochemistry and electron transport rate. The stimulation induced by this substance on gas exchange can be explained by the favourable conditions detected for stomatal density, stomatal index, palisade parenchyma and spongy parenchyma, enhancing the carbon dioxide diffusion in the chloroplasts. Finally, an interesting result found in this research is related to 24-epibrassinolide application on leaves promoting beneficial effects on root anatomy, validating the systemic action of this steroid.

Acknowledgements This research had financial supports from Fundação Amazônia de Amparo a Estudos e Pesquisas (FAPESPA/Brazil), Conselho Nacional de Desenvolvimento Científico e Tecnológico (CNPq/Brazil), Programa de Pós-Graduação em Agronomia (PGAGRO/Brazil) and Universidade Federal Rural da Amazônia (UFRA/Brazil) to AKSL. In other hand, LRS was supported with scholarship from Coordenação de Aperfeiçoamento de Pessoal de Nível Superior (CAPES/Brazil).

Author Contribution Statement AKSL was the advisor of this project, planning all phases of this research. LRS conducted the experiment in the greenhouse and performed physiological, biochemical and morphological determinations, while BRSS measured anatomical parameters. TP and BLB performed nutritional determinations and helped in drafting the manuscript and in interpreting the results.

Data Availability Statement Data are available upon request to the corresponding author.

Compliance with Ethical Standards

Conflict of Interest The authors declare that they have no competing interests.

References

Abdullahi BA, Gu X, Gan Q, Yang Y (2003) Brassinolide amelioration of aluminum toxicity in mungbean seedling growth. J Plant Nutr 26: 1725–1734. https://doi.org/10.1081/PLN-120023278

Abreu IA, Cabelli DE (2010) Superoxide dismutases—a review of the metal-associated mechanistic variations. Biochim Biophys Acta, Proteins Proteomics 1804:263–274. https://doi.org/10.1016/j.bbapap.2009.11.005

Ahammed GJ, Choudhary SP, Chen S et al (2013) Role of brassinosteroids in alleviation of phenanthrene–cadmium co-contamination-induced photosynthetic inhibition and oxidative stress in tomato. J Exp Bot 64:199–213. https://doi.org/10.1093/jxb/ers323

Allen LH Jr, Zhang L, Boote KJ, Hauser BA (2018) Elevated temperature intensity, timing, and duration of exposure affect soybean internode elongation, mainstem node number, and pod number per plant. Crop J 6:148–161. https://doi.org/10.1016/j.cj.2017.10.005

Alyemeni MN, Al-Quwaiz SM (2016) Effect of 28-homobrassinolide on the performance of sensitive and resistant varieties of Vigna radiata. Saudi J Biol Sci 23:698–705. https://doi.org/10.1016/j.sjbs.2016.01.002

Andrejić G, Gajić G, Prica M, Dželetović Ž, Rakić T (2018) Zinc accumulation, photosynthetic gas exchange, and chlorophyll a fluorescence in Zn-stressed Miscanthus × giganteus plants. Photosynthetica 56:1249–1258. https://doi.org/10.1007/s11099-018-0827-3

Antoniadis V, Shaheen SM, Tsadilas CD et al (2018) Zinc sorption by different soils as affected by selective removal of carbonates and hydrous oxides. Appl Geochem 88:49–58. https://doi.org/10.1016/j.apgeochem.2017.04.007

Anwar A, Liu Y, Dong R, Bai L, Yu X, Li Y (2018) The physiological and molecular mechanism of brassinosteroid in response to stress: a review. Biol Res 51:1–15. https://doi.org/10.1186/s40659-018-0195-2

Aragão RM, Silva EN, Vieira CF, Silveira JAG (2012) High supply of NO3 − mitigates salinity effects through an enhancement in the efficiency of photosystem II and CO2 assimilation in Jatropha curcas plants. Acta Physiol Plant 34:2135–2143. https://doi.org/10.1007/s11738-012-1014-y

Arrivault S, Senger T, Krämer U (2006) The Arabidopsis metal tolerance protein AtMTP3 maintains metal homeostasis by mediating Zn exclusion from the shoot under Fe deficiency and Zn oversupply. Plant J 46:861–879. https://doi.org/10.1111/j.1365-313X.2006.02746.x

Azhar N, Su N, Shabala L, Shabala S (2017) Exogenously applied 24-epibrassinolide (EBL) ameliorates detrimental effects of salinity by reducing K+ efflux via depolarization-activated K+ channels. Plant Cell Physiol 58:802–810. https://doi.org/10.1093/pcp/pcx026

Azzarello E, Pandolfi C, Giordano C et al (2012) Ultramorphological and physiological modifications induced by high zinc levels in

Paulownia tomentosa. Environ Exp Bot 81:11–17. https://doi.org/10.1016/j.envexpbot.2012.02.008

Badawi GH, Yamauchi Y, Shimada E et al (2004) Enhanced tolerance to salt stress and water deficit by overexpressing superoxide dismutase in tobacco (Nicotiana tabacum) chloroplasts. Plant Sci 166:919–928. https://doi.org/10.1016/j.plantsci.2003.12.007

Baig MA, Ahmad J, Bagheri R, Ali AA, al-Huqail AA, Ibrahim MM, Qureshi MI (2018) Proteomic and ecophysiological responses of soybean (Glycine max L.) root nodules to Pb and hg stress. BMC Plant Biol 18:283–221. https://doi.org/10.1186/s12870-018-1499-7

Bajguz A (2000) Effect of brassinosteroids on nucleic acids and protein content in cultured cells of Chlorella vulgaris. Plant Physiol Biochem 38:209–215. https://doi.org/10.1016/S0981-9428(00)00733-6

Bajguz A (2010) An enhancing effect of exogenous brassinolide on the growth and antioxidant activity in Chlorella vulgaris cultures under heavy metals stress. Environ Exp Bot 68:175–179. https://doi.org/10.1016/j.envexpbot.2009.11.003

Bajguz A, Hayat S (2009) Effects of brassinosteroids on the plant responses to environmental stresses. Plant Physiol Biochem 47:1–8. https://doi.org/10.1016/j.plaphy.2008.10.002

Balasaraswathi K, Jayaveni S, Sridevi J et al (2017) Cr–induced cellular injury and necrosis in Glycine max L.: biochemical mechanism of oxidative damage in chloroplast. Plant Physiol Biochem 118:653–666. https://doi.org/10.1016/j.plaphy.2017.08.001

Barberon M, Vermeer JEM, De Bellis D et al (2016) Adaptation of root function by nutrient-induced plasticity of endodermal differentiation. Cell 164:447–459. https://doi.org/10.1016/j.cell.2015.12.021

Bazihizina N, Taiti C, Marti L et al (2014) Zn2+−induced changes at the root level account for the increased tolerance of acclimated tobacco plants. J Exp Bot 65:4931–4942. https://doi.org/10.1093/jxb/eru251

Billard V, Maillard A, Garnica M et al (2015) Zn deficiency in Brassica napus induces Mo and Mn accumulation associated with chloroplast proteins variation without Zn remobilization. Plant Physiol Biochem 86:66–71. https://doi.org/10.1016/j.plaphy.2014.11.005

Bradford MM (1976) A rapid and sensitive method for the quantitation of microgram quantities of protein utilizing the principle of protein-dye binding. Anal Biochem 72:248–254. https://doi.org/10.1016/0003-2697(76)90527-3

Cakmak I, Horst WJ (1991) Effect of aluminium on lipid peroxidation, superoxide dismutase, catalase, and peroxidase activities in root tips of soybean (Glycine max). Physiol Plant 83:463–468. https://doi.org/10.1111/j.1399-3054.1991.tb00121.x

Cakmak I, Marschner H (1992) Magnesium deficiency and high light intensity enhance activities of superoxide dismutase, ascorbate peroxidase, and glutathione reductase in bean leaves. Plant Physiol 98:1222–1227. https://doi.org/10.1104/pp.98.4.1222

Casson SA, Hetherington AM (2012) GSK3-like kinases integrate brassinosteroid signaling and stomatal development. Sci Signal 5:1–3. https://doi.org/10.1126/scisignal.2003311

Castro EM, Pereira FJ, Paiva R (2009) Plant histology: structure and function of vegetative organs. Lavras

Cui H (2015) Cortex proliferation in the root is a protective mechanism against abiotic stress. Plant Signal Behav 10:e1011949. https://doi.org/10.1080/15592324.2015.1011949

Dobrikova AG, Vladkova RS, Rashkov GD et al (2014) Effects of exogenous 24-epibrassinolide on the photosynthetic membranes under non-stress conditions. Plant Physiol Biochem 80:75–82. https://doi.org/10.1016/j.plaphy.2014.03.022

Elstner EF, Heupel A (1976) Inhibition of nitrite formation from hydroxylammoniumchloride: a simple assay for superoxide dismutase. Anal Biochem 70:616–620. https://doi.org/10.1016/0003-2697(76)90488-7

Ennajeh M, Vadel AM, Cochard H, Khemira H (2010) Comparative impacts of water stress on the leaf anatomy of a drought-resistant and a drought-sensitive olive cultivar. J Hortic Sci Biotechnol 85:289–294. https://doi.org/10.1080/14620316.2010.11512670

Enstone DE, Peterson CA, Ma F (2003) Root endodermis and exodermis: structure, function, and responses to the environment. J Plant Growth Regul 21:335–351. https://doi.org/10.1007/s00344-003-0002-2

Fan M, Zhu J, Richards C et al (2003) Physiological roles for aerenchyma in phosphorus-stressed roots. Funct Plant Biol 30:493–506. https://doi.org/10.1071/FP03046

FAO (2018) Food and agriculture organization of the united nations. Food outlook: Biannual report on global food markets. FAO, Rome

Fei X, Xing-zheng F, Nan-qi W et al (2016) Physiological changes and expression characteristics of ZIP family genes under zinc deficiency in navel orange (Citrus sinensis). J Integr Agric 15:803–811. https://doi.org/10.1016/S2095-3119(15)61276-X

Fiedor L, Kania A, Mysliwa-Kurdziel B et al (2008) Understanding chlorophylls: central magnesium ion and phytyl as structural determinants. Biochim Biophys Acta Bioenerg 1777:1491–1500. https://doi.org/10.1016/j.bbabio.2008.09.005

Flexas J, Ribas-carbó M, Diaz-espejo A et al (2008) Mesophyll conductance to CO 2 : current knowledge and future prospects. Plant Cell Environ 31:602–621. https://doi.org/10.1111/j.1365-3040.2007.01757.x

Flexas J, Barbour MM, Brendel O et al (2012) Mesophyll diffusion conductance to CO2: an unappreciated central player in photosynthesis. Plant Sci 193–194:70–84. https://doi.org/10.1016/j.plantsci.2012.05.009

Fu C, Li M, Zhang Y et al (2015) Morphology, photosynthesis, and internal structure alterations in field apple leaves under hidden and acute zinc deficiency. Sci Hortic (Amsterdam) 193:47–54. https://doi.org/10.1016/j.scienta.2015.06.016

Gallego SM, Pena LB, Barcia RA et al (2012) Unravelling cadmium toxicity and tolerance in plants: insight into regulatory mechanisms. Environ Exp Bot 83:33–46. https://doi.org/10.1016/j.envexpbot.2012.04.006

Giannopolitis CN, Ries SK (1977) Superoxide dismutases: I. occurrence in higher plants. Plant Physiol 59:309–314

Gong M, Li Y-J, Chen S-Z (1998) Abscisic acid-induced thermotolerance in maize seedlings is mediated by calcium and associated with antioxidant systems. J Plant Physiol 153:488–496. https://doi.org/10.1016/S0176-1617(98)80179-X

Hafeez B, Khanif YM, Saleem M (2013) Role of zinc in plant nutrition- a review. Am J Exp Agric 3:374–391. https://doi.org/10.9734/AJEA/2013/2746

Hajiboland R, Amirazad F (2010) Growth, photosynthesis and antioxidant defense system in Zn-deficient red cabbage plants. Plant Soil Environ 56:209–217

Hameed M, Ashraf M, Naz N (2009) Anatomical adaptations to salinity in cogon grass [Imperata cylindrica (L.) Raeuschel] from the salt range, Pakistan. Plant Soil 322:229–238. https://doi.org/10.1007/s11104-009-9911-6

Hänsch R, Mendel RR (2009) Physiological functions of mineral micronutrients (cu, Zn, Mn, Fe, Ni, Mo, B, cl). Curr Opin Plant Biol 12:259–266. https://doi.org/10.1016/j.pbi.2009.05.006

Hasan SA, Hayat S, Ahmad A (2011) Brassinosteroids protect photosynthetic machinery against the cadmium induced oxidative stress in two tomato cultivars. Chemosphere 84:1446–1451. https://doi.org/10.1016/j.chemosphere.2011.04.047

Havir EA, McHale NA (1987) Biochemical and developmental characterization of multiple forms of catalase in tobacco leaves. Plant Physiol 84:450–455. https://doi.org/10.1104/pp.84.2.450

Hayat S, Yadav S, Wani AS et al (2011) Comparative effect of 28-homobrassinolide and 24-epibrassinolide on the growth, carbonic anhydrase activity and photosynthetic efficiency of Lycopersicon esculentum. Photosynthetica 49:397–404. https://doi.org/10.1007/s11099-011-0051-x

Hayat S, Alyemeni MN, Hasan SA (2012) Foliar spray of brassinosteroid enhances yield and quality of Solanum lycopersicum under cadmium stress. Saudi J Biol Sci 19:325–335

He J, Wang Y, Ding H, Ge C (2016) Epibrassinolide confers zinc stress tolerance by regulating antioxidant enzyme responses, osmolytes, and hormonal balance in Solanum melongena seedlings. Brazilian J Bot 39:295–303. https://doi.org/10.1007/s40415-015-0210-6

Hidoto L, Worku W, Mohammed H, Taran B (2017) Effects of zinc application strategy on zinc content and productivity of chickpea grown under zinc deficient soils. J Soil Sci Plant Nutr 17:112–126. https://doi.org/10.4067/S0718-95162017005000009

Hoagland DR, Arnon DI (1950) The water-culture method for growing plants without soil, 2nd edn. California Agricultural Experiment Station, Riverside

Jain R, Srivastava S, Solomon S et al (2010) Impact of excess zinc on growth parameters, cell division, nutrient accumulation, photosynthetic pigments and oxidative stress of sugarcane (Saccharum spp.). Acta Physiol Plant 32:979–986. https://doi.org/10.1007/s11738-010-0487-9

Javelle M, Vernoud V, Rogowsky PM, Ingram GC (2011) Epidermis: the formation and functions of a fundamental plant tissue. New Phytol 189:17–39. https://doi.org/10.1111/j.1469-8137.2010.03514.x

Jia L, Liu Z, Chen W et al (2015) Hormesis effects induced by cadmium on growth and photosynthetic performance in a hyperaccumulator, Lonicera japonica Thunb. J Plant Growth Regul 34:13–21. https://doi.org/10.1007/s00344-014-9433-1

Jiang YP, Cheng F, Zhou YH et al (2012) Interactive effects of CO2 enrichment and brassinosteroid on CO2 assimilation and photosynthetic electron transport in Cucumis sativus. Environ Exp Bot 75:98–106. https://doi.org/10.1016/j.envexpbot.2011.09.002

Karlidag H, Yildirim E, Turan M (2011) Role of 24-epibrassinolide in mitigating the adverse effects of salt stress on stomatal conductance, membrane permeability, and leaf water content, ionic composition in salt stressed strawberry (Fragaria×ananassa). Sci Hortic (Amsterdam) 130:133–140. https://doi.org/10.1016/j.scienta.2011.06.025

Khodamoradi K, Khoshgoftarmanesh AH, Dalir N et al (2015) How do glycine and histidine in nutrient solution affect zinc uptake and root-to-shoot translocation by wheat and triticale? Crop Pasture Sci 66:1105. https://doi.org/10.1071/CP14227

Kim T, Wetzstein HY (2003) Cytological and ultrastructural evaluations of zinc deficiency in leaves. J Am Soc Hortic Sci 128:171–175. https://doi.org/10.21273/JASHS.128.2.0171

Kim T-W, Michniewicz M, Bergmann DC, Wang Z-Y (2012) Brassinosteroid regulates stomatal development by GSK3- mediated inhibition of a MAPK pathway. Nature 482:419–422. https://doi.org/10.1038/nature10794.Brassinosteroid

Kosesakal T, Unal M (2009) Role of zinc deficiency in photosynthentic pigments and peroxidase activity of tomato seedlings. Istanbul Univ Fac Sci J Biol 68:113–120

Kozhevnikova AD, Seregin IV, Erlikh NT et al (2014) Histidine-mediated xylem loading of zinc is a species-wide character in Noccaea caerulescens. New Phytol 203:508–519. https://doi.org/10.1111/nph.12816

Kumari A, Sheokand S, Swaraj K (2010) Nitric oxide induced alleviation of toxic effects of short term and long term cd stress on growth, oxidative metabolism and cd accumulation in chickpea. Braz J Plant Physiol 22:271–284. https://doi.org/10.1590/S1677-04202010000400007

Kunert KJ, Vorster BJ, Fenta BA et al (2016) Drought stress responses in soybean roots and nodules. Front Plant Sci 7:1–7. https://doi.org/10.3389/fpls.2016.01015

Li M, Ahammed GJ, Li C et al (2016a) Brassinosteroid ameliorates zinc oxide nanoparticles-induced oxidative stress by improving antioxidant potential and redox homeostasis in tomato seedling. Front Plant Sci 7:1–13. https://doi.org/10.3389/fpls.2016.00615

Li X, Guo X, Zhou Y et al (2016b) Overexpression of a brassinosteroid biosynthetic gene dwarf enhances photosynthetic capacity through activation of Calvin cycle enzymes in tomato. BMC Plant Biol 16:33–12. https://doi.org/10.1186/s12870-016-0715-6

Lichtenthaler HK, Buschmann C (2001) Chlorophylls and carotenoids: measurement and characterization by UV-VIS spectroscopy. In: Current protocols in food analytical chemistry. Wiley, Hoboken, pp 431–438

Lima JV, Lobato AKS (2017) Brassinosteroids improve photosystem II efficiency, gas exchange, antioxidant enzymes and growth of cowpea plants exposed to water deficit. Physiol Mol Biol Plants 23:59–72. https://doi.org/10.1007/s12298-016-0410-y

Lima MDR, Barros Junior UO, Batista BL, Lobato AKS (2018) Brassinosteroids mitigate iron deficiency improving nutritional status and photochemical efficiency in Eucalyptus urophylla plants. Trees 32:1681–1694. https://doi.org/10.1007/s00468-018-1743-7

Lynch JP (2007) Rhizoeconomics: the roots of shoot growth limitations. Hortscience 42:1107–1109

Ma JF, Mitani N, Nagao S et al (2004) Characterization of the silicon uptake system and molecular mapping of the silicon transporter gene in rice. Plant Physiol 136:3284–3289. https://doi.org/10.1104/pp.104.047365

Maia CF, Silva BRS, Lobato AKS (2018) Brassinosteroids positively modulate growth: physiological, biochemical and anatomical evidence using two tomato genotypes contrasting to dwarfism. J Plant Growth Regul 37:1–14. https://doi.org/10.1007/s00344-018-9802-2

Manaf A, Raheel M, Sher A et al (2019) Interactive effect of zinc fertilization and cultivar on yield and nutritional attributes of canola (Brassica napus L.). J Soil Sci Plant Nutr 19:in press. https://doi.org/10.1007/s42729-019-00067-2

Marques MC, Nascimento CWA, da Silva AJ, da Silva G-NA (2017) Tolerance of an energy crop (Jatropha curcas L.) to zinc and lead assessed by chlorophyll fluorescence and enzyme activity. South African J Bot 112:275–282. https://doi.org/10.1016/j.sajb.2017.06.009

Martins JPR, Verdoodt V, Pasqual M, De Proft M (2015) Impacts of photoautotrophic and photomixotrophic conditions on in vitro propagated Billbergia zebrina (Bromeliaceae). Plant Cell Tissue Organ Cult 123:121–132. https://doi.org/10.1007/s11240-015-0820-5

Mateos-Naranjo E, Pérez-Romero JA, Redondo-Gómez S et al (2018) Salinity alleviates zinc toxicity in the saltmarsh zinc-accumulator Juncus acutus. Ecotoxicol Environ Saf 163:478–485. https://doi.org/10.1016/j.ecoenv.2018.07.092

Mattiello EM, Ruiz HA, Neves JCL et al (2015) Zinc deficiency affects physiological and anatomical characteristics in maize leaves. J Plant Physiol 183:138–143. https://doi.org/10.1016/j.jplph.2015.05.014

Meyer CJ, Peterson CA, Steudle E (2011) Permeability of Iris germanica's multiseriate exodermis to water, NaCl, and ethanol. J Exp Bot 62:1911–1926. https://doi.org/10.1093/jxb/erq380

Müssig C (2005) Brassinosteroid-promoted growth. Plant Biol 7:110–117. https://doi.org/10.1055/s-2005-837493

Nagajyoti PC, Lee KD, Sreekanth TVM (2010) Heavy metals, occurrence and toxicity for plants: a review. Environ Chem Lett 8:199–216. https://doi.org/10.1007/s10311-010-0297-8

Nakano Y, Asada K (1981) Hydrogen peroxide is scavenged by ascorbate-specific peroxidase in spinach chloroplasts. Plant Cell Physiol 22:867–880

Nisa Z, Chen C, Yu Y et al (2016) Constitutive overexpression of myo-inositol-1-phosphate synthase gene (GsMIPS2) from Glycine soja confers enhanced salt tolerance at various growth stages in Arabidopsis. J Northeast Agric Univ (English Ed 23:28–44. https://doi.org/10.1016/S1006-8104(16)30045-9

Noulas C, Tziouvalekas M, Karyotis T (2018) Zinc in soils, water and food crops. J Trace Elem Med Biol 49:252–260. https://doi.org/10.1016/j.jtemb.2018.02.009

O'Brien TP, Feder N, McCully ME (1964) Polychromatic staining of plant cell walls by toluidine blue O. Protoplasma 59:368–373

Ogweno JO, Song XS, Shi K et al (2008) Brassinosteroids alleviate heat-induced inhibition of photosynthesis by increasing carboxylation efficiency and enhancing antioxidant systems in Lycopersicon esculentum. J Plant Growth Regul 27:49–57. https://doi.org/10.1007/s00344-007-9030-7

Oh K, Yamada K, Asami T, Yoshizawa Y (2012) Synthesis of novel brassinosteroid biosynthesis inhibitors based on the ketoconazole scaffold. Bioorg Med Chem Lett 22:1625–1628. https://doi.org/10.1016/j.bmcl.2011.12.120

Oliveira VP, Lima MDR, Silva BRS et al (2019) Brassinosteroids confer tolerance to salt stress in Eucalyptus urophylla plants enhancing homeostasis, antioxidant metabolism and leaf anatomy. J Plant Growth Regul 19 In press. https://doi.org/10.1007/s00344-018-9870-3

Ouni Y, Mateos-Naranjo E, Abdelly C, Lakhdar A (2016) Interactive effect of salinity and zinc stress on growth and photosynthetic responses of the perennial grass, Polypogon monspeliensis. Ecol Eng 95:171–179. https://doi.org/10.1016/j.ecoleng.2016.06.067

Palmer CM, Guerinot ML (2009) Facing the challenges of cu, Fe and Zn homeostasis in plants. Nat Chem Biol 5:333–340. https://doi.org/10.1038/nchembio.166

Pascual MB, Echevarria V, Gonzalo MJ, Hernández-Apaolaza L (2016) Silicon addition to soybean (Glycine max L.) plants alleviate zinc deficiency. Plant Physiol Biochem 108:132–138. https://doi.org/10.1016/j.plaphy.2016.07.008

Pereira YC, Rodrigues WS, Lima EJA et al (2019) Brassinosteroids increase electron transport and photosynthesis in soybean plants under water deficit. Photosynthetica 57:1–11

Postma JA, Lynch JP (2011) Root cortical aerenchyma enhances the growth of maize on soils with suboptimal availability of nitrogen, phosphorus, and potassium. Plant Physiol 156:1190–1201. https://doi.org/10.1104/pp.111.175489

Rajewska I, Talarek M, Bajguz A (2016) Brassinosteroids and response of plants to heavy metals action. Front Plant Sci 7:1–5. https://doi.org/10.3389/fpls.2016.00629

Ramakrishna B, Rao SSR (2012) 24-Epibrassinolide alleviated zinc-induced oxidative stress in radish (Raphanus sativus L.) seedlings by enhancing antioxidative system. Plant Growth Regul 68:249–259. https://doi.org/10.1007/s10725-012-9713-3

Ramakrishna B, Rao SSR (2015) Foliar application of brassinosteroids alleviates adverse effects of zinc toxicity in radish (Raphanus sativus L.) plants. Protoplasma 252:665–677. https://doi.org/10.1007/s00709-014-0714-0

Reis AR, Lisboa LAM, Reis HPG et al (2018) Depicting the physiological and ultrastructural responses of soybean plants to Al stress conditions. Plant Physiol Biochem 130:377–390. https://doi.org/10.1016/j.plaphy.2018.07.028

Rezapour S, Golmohammad H, Ramezanpour H (2014) Impact of parent rock and topography aspect on the distribution of soil trace metals in natural ecosystems. Int J Environ Sci Technol 11:2075–2086. https://doi.org/10.1007/s13762-014-0663-3

Sadeghzadeh B (2013) A review of zinc nutrition and plant breeding. J Soil Sci Plant Nutr 13:905–927. https://doi.org/10.4067/S0718-95162013005000072

Saengwilai P, Nord EA, Chimungu JG et al (2014) Root cortical aerenchyma enhances nitrogen acquisition from low-nitrogen soils in maize. Plant Physiol 166:726–735. https://doi.org/10.1104/pp.114.241711

Sagardoy R, Morales F, López-Millán AF et al (2009) Effects of zinc toxicity on sugar beet (Beta vulgaris L.) plants grown in hydroponics. Plant Biol 11:339–350. https://doi.org/10.1111/j.1438-8677.2008.00153.x

Salama ZA, El-Fouly MM, Lazova G, Popova LP (2006) Carboxylating enzymes and carbonic anhydrase functions were suppressed by zinc deficiency in maize and chickpea plants. Acta Physiol Plant 28:445–451. https://doi.org/10.1007/BF02706627

Samreen T, Humaira, Shah HU et al (2017) Zinc effect on growth rate, chlorophyll, protein and mineral contents of hydroponically grown mungbeans plant (Vigna radiata). Arab J Chem 10:S1802–S1807. https://doi.org/10.1016/j.arabjc.2013.07.005

Santos EF, Santini JMK, Paixão AP et al (2017) Physiological highlights of manganese toxicity symptoms in soybean plants: Mn toxicity responses. Plant Physiol Biochem 113:6–19. https://doi.org/10.1016/j.plaphy.2017.01.022

Santos LR, Batista BL, Lobato AKS (2018) Brassinosteroids mitigate cadmium toxicity in cowpea plants. Photosynthetica 56:591–605. https://doi.org/10.1007/s11099-017-0700-9

Schneider HM, Wojciechowski T, Postma JA et al (2017) Root cortical senescence decreases root respiration, nutrient content and radial water and nutrient transport in barley. Plant Cell Environ 40:1392–1408. https://doi.org/10.1111/pce.12933

Segatto FB, Bisognin DA, Benedetti M et al (2004) A technique for the anatomical study of potato leaf epidermis. Ciência Rural 34:1597–1601. https://doi.org/10.1590/S0103-84782004000500042

Shahbaz M, Ashraf M, Athar H-U-R (2008) Does exogenous application of 24-epibrassinolide ameliorate salt induced growth inhibition in wheat (Triticum aestivum L.)? Plant Growth Regul 55:51–64. https://doi.org/10.1007/s10725-008-9262-y

Shu S, Tang Y, Yuan Y et al (2016) The role of 24-epibrassinolide in the regulation of photosynthetic characteristics and nitrogen metabolism of tomato seedlings under a combined low temperature and weak light stress. Plant Physiol Biochem 107:344–353. https://doi.org/10.1016/j.plaphy.2016.06.021

Shu K, Qi Y, Chen F et al (2017) Salt stress represses soybean seed germination by negatively regulating GA biosynthesis while positively mediating ABA biosynthesis. Front Plant Sci 8:1–12. https://doi.org/10.3389/fpls.2017.01372

Siddiqui H, Ahmed KBM, Hayat S (2018) Comparative effect of 28-homobrassinolide and 24-epibrassinolide on the performance of different components influencing the photosynthetic machinery in Brassica juncea L. Plant Physiol Biochem 129:198–212. https://doi.org/10.1016/j.plaphy.2018.05.027

Silva EN, Ribeiro RV, Ferreira-Silva SL et al (2012) Coordinate changes in photosynthesis, sugar accumulation and antioxidative enzymes improve the performance of Jatropha curcas plants under drought stress. Biomass Bioenergy 45:270–279. https://doi.org/10.1016/j.biombioe.2012.06.009

Sinclair SA, Krämer U (2012) The zinc homeostasis network of land plants. Biochim Biophys Acta, Mol Cell Res 1823:1553–1567. https://doi.org/10.1016/j.bbamcr.2012.05.016

Singh HP, Batish DR, Kohli RK, Arora K (2007) Arsenic-induced root growth inhibition in mung bean (Phaseolus aureus Roxb.) is due to oxidative stress resulting from enhanced lipid peroxidation. Plant Growth Regul 53:65–73. https://doi.org/10.1007/s10725-007-9205-z

Singh P, Kumar R, Sabapathy SN, Bawa AS (2008) Functional and edible uses of soy protein products. Compr Rev Food Sci Food Saf 7:14–28. https://doi.org/10.1111/j.1541-4337.2007.00025.x

Singh P, Shukla AK, Behera SK, Tiwari PK (2019) Zinc application enhances superoxide dismutase and carbonic anhydrase activities in zinc-efficient and zinc-inefficient wheat genotypes. J soil Sci plant Nutr 19:in press. https://doi.org/10.1007/s42729-019-00038-7

Steel RG, Torrie JH, Dickey DA (2006) Principles and procedures of statistics: a biometrical approach, 3rd edn. Academic Internet Publishers, Moorpark

Subba P, Mukhopadhyay M, Mahato SK, Bhutia KD, Mondal TK, Ghosh SK (2014) Zinc stress induces physiological, ultra-structural and biochemical changes in mandarin orange (Citrus reticulata Blanco) seedlings. Physiol Mol Biol Plants 20:461–473. https://doi.org/10.1007/s12298-014-0254-2

Suhr N, Schoenberg R, Chew D et al (2018) Elemental and isotopic behaviour of Zn in Deccan basalt weathering profiles: chemical weathering from bedrock to laterite and links to Zn deficiency in tropical soils. Sci Total Environ 619–620:1451–1463. https://doi.org/10.1016/j.scitotenv.2017.11.112

Swamy KN, Rao SSR (2009) Effect of 24-epibrassinolide on growth, photosynthesis, and essential oil content of Pelargonium graveolens (L.) Herit. Russ J Plant Physiol 56:616–620. https://doi.org/10.1134/S1021443709050057

Tadayon MS, Moafpourian G (2019) Effects of exogenous epibrassinolid, zinc and boron foliar nutrition on fruit development and ripening of grape (Vitis vinifera L. clv. "Khalili"). Sci Hortic (Amsterdam) 244:94–101. https://doi.org/10.1016/j.scienta.2018.09.036

Talukdar D (2013) Arsenic-induced oxidative stress in the common bean legume, Phaseolus vulgaris L. seedlings and its amelioration by exogenous nitric oxide. Physiol Mol Biol Plants 19:69–79. https://doi.org/10.1007/s12298-012-0140-8

Tanaka N, Kato M, Tomioka R et al (2014) Characteristics of a root hairless line of Arabidopsis thaliana under physiological stresses. J Exp Bot 65:1497–1512. https://doi.org/10.1093/jxb/eru014

Tavallali V, Rahemi M, Maftoun M et al (2009) Zinc influence and salt stress on photosynthesis, water relations, and carbonic anhydrase activity in pistachio. Sci Hortic (Amsterdam) 123:272–279. https://doi.org/10.1016/j.scienta.2009.09.006

Thussagunpanit J, Jutamanee K, Sonjaroon W et al (2015) Effects of brassinosteroid and brassinosteroid mimic on photosynthetic efficiency and rice yield under heat stress. Photosynthetica 53:312–320. https://doi.org/10.1007/s11099-015-0106-5

Tripathi DK, Singh S, Singh S, Mishra S, Chauhan DK, Dubey NK (2015) Micronutrients and their diverse role in agricultural crops: advances and future prospective. Acta Physiol Plant 37:14–14. https://doi.org/10.1007/s11738-015-1870-3

Velikova V, Yordanov I, Edreva A (2000) Oxidative stress and some antioxidant systems in acid rain-treated bean plants protective role of exogenous polyamines. Plant Sci 151:59–66. https://doi.org/10.1016/S0168-9452(99)00197-1

Wang X, Zhao X, Jiang C et al (2015) Effects of potassium deficiency on photosynthesis and photoprotection mechanisms in soybean (Glycine max (L.) Merr.). J Integr Agric 14:856–863. https://doi.org/10.1016/S2095-3119(14)60848-0

Wei Z, Li J (2016) Brassinosteroids regulate root growth, development, and Symbiosis. Mol Plant 9:86–100. https://doi.org/10.1016/j.molp.2015.12.003

Wijewardana C, Reddy KR, Bellaloui N (2019) Soybean seed physiology, quality, and chemical composition under soil moisture stress. Food Chem 278:92–100. https://doi.org/10.1016/j.foodchem.2018.11.035

Wu Q-S, Xia R-X, Zou Y-N (2006) Reactive oxygen metabolism in mycorrhizal and non-mycorrhizal citrus (Poncirus trifoliata) seedlings subjected to water stress. J Plant Physiol 163:1101–1110. https://doi.org/10.1016/j.jplph.2005.09.001

Xia X-J, Huang L-F, Zhou Y-H et al (2009) Brassinosteroids promote photosynthesis and growth by enhancing activation of Rubisco and expression of photosynthetic genes in Cucumis sativus. Planta 230:1185–1196. https://doi.org/10.1007/s00425-009-1016-1

Yu JQ, Huang L-F, Hu WH et al (2004) A role for brassinosteroids in the regulation of photosynthesis in Cucumis sativus. J Exp Bot 55:1135–1143. https://doi.org/10.1093/jxb/erh124

Yuan L, Zhu S, Shu S et al (2015) Regulation of 2,4-epibrassinolide on mineral nutrient uptake and ion distribution in Ca(NO3)2 stressed cucumber plants. J Plant Physiol 188:29–36. https://doi.org/10.1016/j.jplph.2015.06.010

Zhang YP, Zhu XH, Ding HD et al (2013) Foliar application of 24-epibrassinolide alleviates high-temperature-induced inhibition of photosynthesis in seedlings of two melon cultivars. Photosynthetica 51:341–349. https://doi.org/10.1007/s11099-013-0031-4

Zhang Y, Xu S, Yang S, Chen Y (2015) Salicylic acid alleviates cadmium-induced inhibition of growth and photosynthesis through upregulating antioxidant defense system in two melon cultivars (Cucumis melo L.). Protoplasma 252:911–924. https://doi.org/10.1007/s00709-014-0732-y

Zhiponova MK, Vanhoutte I, Boudolf V et al (2013) Brassinosteroid production and signaling differentially control cell division and expansion in the leaf. New Phytol 197:490–502. https://doi.org/10.1111/nph.12036